SYNTHESIS AND CHARACTERIZATION OF BOVINE SERUM ALBUMIN BASED NANOCONTAINERS FOR DRUG DELIVERY APPLICATIONS

by

Elif Özlem Topal

B.S. , Physics, Middle East Technical University, 2019

B.S. , Molecular Biology and Genetics, Cumhuriyet University, 2011

Submitted to the Institute of Biomedical Engineering

in partial fulfillment of the requirements

for the degree of

Master of Science

in

Biomedical Engineering

Boğaziçi University

2023

SYNTHESIS AND CHARACTERIZATION OF BOVINE SERUM ALBUMIN BASED NANOCONTAINERS FOR DRUG DELIVERY APPLICATIONS

APPROVED BY:

Assist. Prof. Dr. Banu İyisan (Thesis Advisor)	.....
Prof. Dr. Bora Garipcan	.....
Assist. Prof. Dr. Nebahat Aral-Yılmaz	.....

DATE OF APPROVAL: 11.01.2023

ACKNOWLEDGMENTS

First of all, I would like to thank my advisor Assist. Prof. Dr. Banu İyisan for her support and beneficial advice during my thesis studies. I also would like to thank my friends Research Assistant Sedef Salel, Hayriye Öztatlı and Damla Kelle for their help for the laboratory studies. I would also like to thank my friends Gizem Uysal, Dilan Avşar Akdeniz, and Gökçen Boran for their friendship and support.

I also would like to thank my friends Bülent Sevinç, Sinan Çelik and Aykut Hınık for their exhortation and support during my whole journey.

Lastly, I wish to express my special thanks to my dear mother Cihangül Topal for her support throughout my life.

This thesis funded by the BU Research Fund (18042)

This thesis is dedicated to my beloved father Temur Topal.

january 2023

ACADEMIC ETHICS AND INTEGRITY STATEMENT

I, Elif Özlem Topal, hereby certify that I am aware of the Academic Ethics and Integrity Policy issued by the Council of Higher Education (YÖK) and I fully acknowledge all the consequences due to its violation by plagiarism or any other way.

Name :

Signature:

Date:

ABSTRACT

SYNTHESIS AND CHARACTERIZATION OF BOVINE SERUM ALBUMIN BASED NANOCONTAINERS FOR DRUG DELIVERY APPLICATIONS

Polymeric nanocontainers which consist of both a core and a polymeric membrane have an important role for drug delivery applications. They can carry active compounds like drugs, proteins in their core and their polymeric membrane prevent the living environment from the side effects of these carried compounds. There are various types of polymeric materials that can be natural or synthetic according to their source for the production of the polymeric nanocontainers. Also, the combinations of different polymers are used to produce highly stable nanocontainers. The main goal of this thesis study is fabrication of totally biocompatible, biodegradable, durable, nanocontainers that consist of polymeric shell and lipid core. For these reasons, conjugates made of the Bovine Serum Albumin (BSA) which is a protein and Pectin which is a polysaccharide, were synthesized through the Maillard reaction based on reducing sugar and proteins without using external chemicals or enzyme. The effects of protein- polysaccharide weight ratio, pH adjustment were investigated to optimize the conjugate formulation. The produced conjugates were characterized via Protein Assay, SDS-PAGE and FT-IR Analysis. The polymeric nanocontainers were produced through oil-in-water miniemulsion method by using the obtained BSA and Pectin conjugates. Addition of biocompatible stabilizers had a drastic influence on the resulting features on the nanocontainers which are extensively characterized by dynamic light scattering analysis, zeta potential measurements and STEM imaging.

Keywords: Biopolymeric Nanocontainer, Maillard Reaction, BSA-Pectin Conjugates

ÖZET

İLAÇ SALIMI UYGULAMALARI İÇİN SIĞIR SERUM ALBUMİN BAZLI NANOPARTİKÜLLERİN SENTEZİ VE KARAKTERİZASYONU

Bir çekirdek ve bir de polimerik membrandan oluşan polimerik nanopartiküller, ilaç salım uygulamalarında önemli bir role sahiptir. Nanopartiküller çekirdeklerinde ilaç, protein gibi aktif bileşikleri taşıyabilirler ve polimerik membran canlı ortamını bu taşınan bileşiklerin yan etkilerinden korur. Polimerik nanopartiküllerin üretimi için kaynağına göre doğal veya sentetik olabilen çeşitli polimer malzemeler bulunmaktadır. Ayrıca, stabilitesi yüksek nanokapsüller üretmek için farklı polimerlerin kombinasyonları da kullanılabilir. Bu tez çalışmasının temel amacı, tamamen biyouyumlu, biyolojik olarak parçalanabilen, dayanıklı, polimerik kabuk ve lipid çekirdekten oluşan nanopartiküllller üretmektir. Bu nedenlerle, bir protein olan Bovine Serum Albumin (BSA) ve bir polisakkarit olan Pektin'den oluşan konjugatlar, ekstra kimyasal veya enzim kullanılmadan polisakkarit ve proteinin indirgenmesine dayalı Maillard reaksiyonu ile sentezlendi. Konjugat formülasyonunu optimize etmek için protein-polisakkarit ağırlık oranı, pH ayarlaması yapmanın etkileri araştırıldı. Üretilen konjugatlar, Protein Assay, SDS-PAGE ve FT-IR Analizi ile karakterize edildi. Elde edilen BSA ve Pectin konjugatları kullanılarak suda yağ miniemülsiyon yöntemiyle polimerik nanopartiküller üretildi. Biyouyumlu stabilizatörlerin eklenmesi, dinamik ışık saçılımı analizi, zeta potansiyel ölçümleri ve STEM görüntüleme ile kapsamlı bir şekilde karakterize edilen nanopartiküller üzerinde önemli bir etkiye sahipti.

Anahtar Sözcükler: Biyopolimerik Nanopartikül, Maillard Reaksiyonu, BSA-Pektin Konjugatları

TABLE OF CONTENTS

ACKNOWLEDGMENTS iii
ACADEMIC ETHICS AND INTEGRITY STATEMENT iv
ABSTRACT v
ÖZET vi
LIST OF FIGURES ix
LIST OF TABLES xii
LIST OF SYMBOLS xiii
LIST OF ABBREVIATIONS xiv
1. INTRODUCTION 1
2. BACKGROUND 9
2.1 Bovine Serum Albumin (BSA) 9
2.1.1 Structure of the BSA 9
2.1.2 Functional Properties of the BSA 10
2.1.3 Biomedical Applications of the BSA 11
2.2 Pectin 11
2.2.1 Structure of the Pectin 12
2.2.2 Functional Properties of the Pectin 13
2.2.3 Biomedical Applications of the Pectin 14
2.3 BSA-Pectin Maillard Reaction 14
3. MATERIALS AND METHODS 16
3.1 Materials 16
3.2 Preparation of the BSA-Pectin Conjugates via Maillard Reaction . . . 16
3.3 Characterization of the BSA-Pectin Conjugates 17
3.3.1 Protein Assay 18
3.3.2 Sodium Dodecyl Sulfate-Polyacrylamide Gel Electrophoresis (SDS-PAGE) 19
3.3.3 Fourier Transform-Infrared Spectroscopy (FT-IR) Analysis . . . 21
3.4 Nanocontainer Production 21
3.5 Characterization of the Nanocontainers 22

3.5.1 Solid Content Measurement 24
3.5.2 Dynamic Light Scattering (DLS) Measurement 24
3.5.3 Zeta Potential Measurement 24
3.5.4 Scanning Transmission Electron Microscopy (STEM) Imaging . 25
4. RESULTS AND DISCUSSION 27
4.1 Characterization Results of the BSA-Pectin Conjugates 27
4.1.1 Protein Assay 27
4.1.2 Sodium Dodecyl Sulfate-Polyacrylamide Gel Electrophoresis (SDS-PAGE) 29
4.1.3 Fourier Transform- Infrared Spectroscopy (FT-IR) Analysis . . 30
4.2 Characterization Results of the Nanocontainers 32
4.2.1 Dynamic Light Scattering (DLS) Measurements 33
4.2.1.1 Effect of the BSA-Pectin Weight Ratio and Surfactant Usage 33
4.2.1.2 Effect of the pH Adjustment 34
4.2.1.3 Effect of the BSA-Pectin Conjugate Concentration . . 36
4.2.1.4 Effect of the Purification 37
4.2.2 Zeta Potential Measurements 38
4.2.3 Scanning Transmission Electron Microscopy (STEM) Imaging . 39
5. CONCLUSIONS AND OUTLOOK 42
5.1 Conclusions 42
5.2 Outlook 44
REFERENCES 45
APPENDIX A. CALIBRATION CURVE FOR PROTEIN ASSAY 54

LIST OF FIGURES

Figure 1.1	Diagram constructed by the John Hodge to make clear the Maillard reaction network [25].	5
Figure 1.2	Simplified Maillard reaction stages with sub-products information [26].	6
Figure 1.3	Schematic representation of the solvent evaporation method to produce nanoparticles from the preformed polymers [1].	7
Figure 2.1	Schematic representation of the subdomains of the Bovine Serum Albumin and its tryptophan residues [40].	10
Figure 2.2	Cell wall of the plants surrounding and providing tensile strength to plant cell by its three layers which are the middle lamella, primary cell wall and the secondary cell wall (not in the figure) including hemicellulose, cellulose microfibrils, lignin, soluble protein and pectin [46].	12
Figure 2.3	Schematic representation of pectin including the apiogalacturonan (AG), xylogalacturonan (XG), rhamnogalacturonan I (RG-I), rhamnogalacturonan II (RG-II), and homogalacturonan (HG) regions. The main structure constituting the 60% of total pectin is linear, the smooth pectin region is constituted by the moderately esterified homogalacturonan backbone. The many branches of RG I and RG II domains and a few AG and XG extends construct hairy regions. [44].	13
Figure 2.4	Shematic representation of the formation of the BSA-Pectin conjugates via Maillard reaction	15
Figure 3.1	Schematic representation of the overall procedure in this thesis study.	17
Figure 3.2	A) BSA-Pectin conjugates produced without any pH adjustment. B) BSA-Pectin conjugates produced with increased pH value.	18

Figure 3.3 A1) The initial dispersions including nanocontainers produced with solely BSA produced with surfactant and without using surfactant. A2) Dispersions after one month storage period. A3) Dispersions after two month storage period. A4) Dispersions after three month storage period. B1) The initial dispersions including nanocontainers produced with BSA-Pecin conjugate having 2:1 m_{BSA}:m_{Pectin} weight ratio produced with surfactant and without using surfactant. B2) Dispersions after one month storage period. B3) Dispersions after two month storage period. B4) Dispersions after three month storage period. 23

Figure 3.4 A) The initial dispersions including the nanocontainers produced with BSA-Pectin conjugate having 2:1 m_{BSA}:m_{Pectin} weight ratio and prepared at increased pH value by using surfactant and without surfactant. B) The same dispersions one month later 23

Figure 4.1 Image of the SDS-PAGE gel shows the weight ratio distributions of the reference Ladder, only BSA and BSA-Pectin conjugates having 1:7, 1:2, 2:1,7:1 m_{BSA}:m_{Pectin} weight ratios respectively. 29

Figure 4.2 The FT-IR Analysis of the solely BSA (pink curve), solely Pectin (blue curve) and the BSA-Pectin conjugate with 2:1 m_{BSA}:m_{Pectin} weight ratio prepared without making any pH adjustment (red curve). 31

Figure 4.3 The FT-IR Analysis of the solely BSA (pink curve), solely Pectin (blue curve) and the BSA-Pectin conjugate with 2:1 (m_{BSA}:m_{Pectin}) weight ratio prepared with pH adjustment (red curve). 32

Figure 4.4 The size of the nanocontainer vs m_{BSA}:m_{Pectin} weight ratio of the used conjugate to produce the nanocontainer. 34

Figure 4.5 STEM Images of the nanocontainers produced with BSA-Pectin conjugate having 2:1 m_{BSA}:m_{Pectin} weight ratio prepared with pH adjustment by using surfactant A) Scale; 500 nm B) Scale; 500 nm size measurements C) Scale; 100 nm D) Scale; 100 nm size measurement. 40

Figure 4.6 STEM Images of the nanocontainers produced with BSA-Pectin conjugate, having 2:1 m_{BSA}:m_{Pectin} weight ratio prepared with pH adjustment without using surfactant. A) Scale; 500 nm B) Scale; 500 nm size measurements C) Scale; 100 nm D) Scale; 300 nm. 40

Figure 4.7 STEM Images of the syringe filtered nanocontainers produced with BSA-Pectin conjugate having 2:1 m_{BSA}:m_{Pectin} weight ratio prepared with pH adjustment by using surfactant. B. Scale; 300 nm B) The same scale with size measurements C) Scale; 500 nm D) Scale; 500 nm size measurements. 41

Figure A.1 Generated Calibration Curve at $\lambda = 655$ nm by using solutions having different BSA concentration to determine the BSA contration in the produced BSA-Pectin conjugates. 54

LIST OF TABLES

Table 4.1	Results of the protein assay studies on the produced BSA-Pectin Conjugates	28
Table 4.2	Protein Assay results of the BSA-Pectin conjugates (m_{BSA}:m_{Pectin} weight ratio is 2:1) prepared without making any pH adjustment and prepared by increased pH value.	28
Table 4.3	DLS measurement results of the produced nanocontainers.	34
Table 4.4	The DLS measurement results of the nanocontainers produced with the conjugates, having 2:1 m_{BSA}:m_{Pectin} weight ratio prepared by both pH adjustment and without pH adjustment.	35
Table 4.5	The DLS and solid content measurement results of the nanocontainers prepared by using the solution including 1mg/ml, 2mg /ml and 3 mg/ml BSA-Pectin conjugates having 2:1 m_{BSA}:m_{Pectin} weight ratio prepared with increased pH value (pH 8.3).	36
Table 4.6	The DLS and solid content measurement results after the centrifugation process.	37
Table 4.7	The DLS and solid content measurement results after the syringe filtration process.	38
Table 4.8	Zeta potential measurement results	38

LIST OF SYMBOLS

α	Alpha
ϵ	Epsilon
β	Beta
Mg^{2+}	Magnesium (ion)
Ca^{2+}	Calcium (ion)
Zn^{2+}	Zinc (ion)
NaCI	Sodium Chloride
°C	Celcius
μg	Microgram
μL	Microliter
mg	Milligram
V	Volt
%	Percentage
nm	Nanometer

LIST OF ABBREVIATIONS

AGEs	Advanced Glycation end-Products
BSA	Bovine Serum Albumin
CMC	Critical Micelle Concentration
DLS	Dynamic Light Scattering
FL	Fructoselysine
FT-IR	Fourier Transform-Infrared Spectroscopy
IR	Infrared
MRPs	Maillard reaction products
LBL	Layer by Layer
PCL	Polycaprolactone
PDI	Polydispersity Index
PEG	Polyethylene Glycol
PEO	Polyethyleneoxide
PLGA	Poly(Lactic-co-Glycolic Acid)
PVA	Polyvinyl Alcohol
SDS-PAGE	Sodium Dodecyl Sulfate-Polyacrylamide Gel Electrophoresis
STEM	Scanning Transmission Electron Microscopy
TEM	Transmission Electron Microscopy

1. INTRODUCTION

Particles which are in the size range from 1 to 100 nm are named as nanoparticle regardless of their shape [1, 2]. The nanocapsules and nanospheres are sub-types of the nanoparticles and the differences between them come from their architecture and morphology [1]. As a special kind of nanostructure, polymeric nanocapsules are container like structures consist of both a core including some drugs, proteins and polymeric membrane covering the core [3]. The polymeric membrane provides more durable feature to nanocapsule in the extreme conditions like enzyme activity, and pH. It also prevents the living environment from the negative effects of the cargo molecules inside the core while providing the controlled leakage of these molecules into the living environment [4]. These advantageous features of the polymeric nanocapsules make them a leading candidate for the drug delivery applications.

As a drug carrier agent, the polymeric material used for the formation of the nanocapsules should be biocompatible and biodegradable to execute their functions like releasing the compounds inside the nanocapsule and annihilate the capsules from the living organism. Although they are not biodegradable, biocompatible some polymers like polyvinyl alcohol (PVA) and polyethylene glycol (PEG) are broadly used in this field because of their hydrophilic feature enables them release the payload. In addition to these, there are various types of polymeric materials divided into two subgroups which are natural and synthetic polymers depending on their source are used for the production of the polymeric shell of the nanocapsules. As a natural polymeric material polysaccharide such as chitosan, dextran, alginate, dextran sulfate, hyaluronan are widely used in this field [5]. For carrying therapeutic proteins and peptides, as a biocompatible, biodegradable, non-toxic material alginate (anionic) and chitosan (cationic) combination are employed [6]. In addition to these, the chitosan has the ability to interact and remain the ocular mucosa, gastrointestinal tract for a long time, so it is preferred for both ocular and colon-specific drug delivery systems [7]. It also has hemostatic activity, antimicrobial and would healing features [8]. The alginate is useful for the pH- responsive applications because it gives the nanoparticle discharging

the payload in alkaline conditions [5]. The dextran which has a variety of applications with its reducing blood viscosity and preventing formation of blood clots in the medical field is another employed natural polymer [9]. Other natural polymers used to produce the cover of the nanocapsules are protein-based molecules because of their configurable and biocompatible feature [5]. According to application aim, the type of the protein used for the nanocontainer synthesis can be changed, but bovine serum albumin, casein, hemoglobin, and fibrinogen are used widely. In addition to these, soy protein, elastin, silk fibroin, keratin, and collagen are also employed for the production of the nanocontainers [10]. Silk fibroin is a material that can bind to both hydrophilic and hydrophobic drugs and it has mild preparation conditions. Silk fibroin-based nanoparticles enable controlled drug release and improve the therapeutic efficiency of the drugs [10, 11]. The soy protein is also preferred because it allows the usage of the many drugs by its medium concentration of the charged, non-polar, and polar amino acids [12]. Due to their inverse temperature transition feature, elastin polymers are also chosen to produce nanocapsules. They are soluble in the water under a critical temperature, however, when the temperature extends the critical level the chains of the polymers fold hydrophobically [13]. Fibrin based nanocontainers are used to deliver drugs, cells, genes and active biomolecules [14]. For carrying some nutraceuticals like vitamin D3, quercetin, anticancer drugs, omega-3 poly unsaturated fatty acids, curcumin, α-tocopherol and polyphenols casein based nanocontainers are employed [15]. As a most abundant protein the collagen has the ability of repair skin, knee meniscal, bone, joint cartilage, esophagus, muscle, nerves system and dura mater, so its combination with some other materials is used widely in synthesis of the nanocontainers [16]. On the other hand, thanks to their biodegradability and biocompatibility feature, synthetic polymers, aliphatic polyesters and combinations of the different polymers are commonly studied and developed in drug delivery systems [5]. As a polymer polylactic acid (PLA) can undergo scission process in the metabolism to degrade into its monomeric unit lactic acid which is a natural intermediate in the carbohydrate metabolism, so it is used widely in the drug delivery studies [17]. To encapsulate lipophilic drugs poly (lactic-co-glycolic acid) (PLGA) based nanoparticles are employed widely. Additionally, PLGA based nanoparticles increase the drug in tumor cells to highest level and also, they rise the drug concentration in the formulation [18]. In agriculture, especially to carry pes-

ticides and herbicides polycaprolactone nanocapsules (PCL) are used extensively due to their easily synthesizable, high loading capacity, low toxicity, ability of the solving pesticides and herbicides [19]. As a series of synthetic polymer having different proportion of methacrylate and acrylate portions, Eudragit® polymers are used to coat many kinds of dosage of the poorly soluble drugs and drug solid dispersions providing controlled drug release and increasing drug dissolution [5, 20]. Polyethylene glycol (PEG) is a polyether employed in many drug delivery studies. It is soluble in ethanol, benzene, dichloromethane, acetonitrile, however, it is not soluble in the hexane and diethyl ether. Formation of the protein corona can be blocked by PEG with its ability of preventing the protein adsorption, so it is preferred extensively to produce nanocapsules [21]. Beside of these natural and synthetic polymeric materials, the combination of these molecules like PLGA-PEG, PLGA-Chitosan are also used widely to produce nanocapsules having high potential to realize the drug delivery function. In this thesis study, conjugate of the natural polymers including Pectin and Bovine Serum Albumin (BSA) was prepared via the Maillard Reaction and the prepared conjugates were used as nanocontainer's shell material. The Maillard Reaction is at first defined by Louis Camille Maillard (1878–1936) who was French chemist and physicist [22]. The reaction also known as nonenzymatic browning reaction in food sciences because it is based on reducing sugar and proteins by heat without using any extra chemicals [23–25] It is also named as glycoxidation and protein glycation in medical and health sciences [24]. The Maillard reaction identification does not mean just one reaction pathway, it consists of many reactions network based on complex chemistry [25]. The steps of the Maillard reaction products (MRPs), also known as advanced glycation end-products (AGEs), initially described by the American scientist, John Hodge (1914-1996) [24, 25]. The first coherent Maillard reaction scheme, constituted by the Hodge, including 7 steps (A-G). (Figure 1.1) Additionally, by the recognizing of the work regarding the free radical degradation of Maillard intermediates, conducted by the Japanese scientists Namiki and co-workers , in 1986, the H step was added to the initial scheme. (Figure 1.1) For this reason, the step H, involving free radical-mediated formation of carbonyl fission products from the reducing sugar, of the Maillard reaction scheme is named as Namiki pathway [25]. The carbonyl group condensation occurs in the initial stage of the Maillard reaction, to exemplify, a free amino group, generally epsilon amino group

of lysine residues within proteins reduces sugar like glucose. (Step A, Figure 1.1) Amadori product, (1-amino-1-deoxy-2-ketose (ketoamine)) named after the Italian scientist Mario Amadori, is came out after the glycation reaction results in the formation of unstable, spontaneously reaaranged Schiff base (aldimine).(Step B, Figure1.1) At physiological pH, the equilibrium constant to produce Amadori product goes in the forward direction. However, presence of phosphate and inceasing the pH value causes increase in the reversibility. In Step C to Step D (Figure 1.1) to form the furfurals, fragmentation products (carbonyl and hydroxycarbonyl compounds) and reductones Amadori product is reduced in many pathways. The compounds can be also formed from the sugar directly without use of the amino groups coming from the protein. Thanks to alkaline setting, the reductons are produced, but acidic media helps the formation of furfurals in Step C. (Figure 1.1) The enediol intermediates can catalyze redox reactions according to recycling of transition metals like iron, copper, so they have equal reducing power. However, they can show antioxidant activity like ascorbate. By retroaldolization the sugar fragmentation occurs in Step D. (Figure 1.1) To give Strecker aldehydes of aminoketones and amino acids; Dicarbonyl compounds like methylglyoxal, butanedione, glyoxal formed in this step can react with amino acids by favor of the Strecker degradation in Step E. (Figure 1.1) The final stage of the Maillard reaction is summarized in Step F and Step G. (Figure 1.1) In these steps, the color formation is occurred with many compounds that can be larger polymeric materials (protein-polysaccharide conjugate) or small molecules [25, 26]. There are many studies published on the reaction, but to simplify the whole process the Maillard reaction subdivided into mainly three categories in these studies [22, 26].(Figure 1.2) The two reactions sugar and amine condensation (Step A, Figure 1.1) and Amadori product rearrangement (Step B, Figure 1.1) are commentated in the initial or early stage that is not seen any color change. In early stage, the nutritional value can be decreased because of the decrease in availability of the amino acid [26]. Degradation of sugar (Step C, Figure 1.1), fragmentation (Step D, Figure 1.1) and amino acid degradation (Step E, Figure 1.1) occur in the intermediate or advanced stage. In the advanced stage the color of the product can change slightly to yellow. When the process come to the final stage the color of the product becomes darker, and the condensation of aldols (Step F, Figure 1.1), condensation of aldehyde-amine, formation of heterocyclic

nitrogen compounds (Step G, Figure 1.1) reactions are seen, and so the polymeric compounds (protein-polysaccharide conjugate) are produced [27]. To produce foods having better taste and appearance the Maillard reaction has been preferred for thousands of years while cooking the foods. To produce many foods, which need the better flavor and color to meet the consumers' demand, like bakery products, coffee, chocolate, the manufacturing processes in the modern food industry includes many applications of the Maillard reaction [28, 29]. In humid substances in the sea and the soil it has a complex role. Amino acids compound coming out from the plant litter interact with lignin and humid substances are formed. Formation of humid substances from the condensation of sugars with molecules produced from the plant litter recognized by the Maillard. The Maillard reaction also takes place in the textiles specially to decrease the yellowing problem during the storage. By using the reaction with reducing the sugars, wool can be modified in the textile industry. On prolonged storage, decomposition of some pharmaceutical preparations the Maillard reaction has an important role [29].

Products of the Maillard reaction increase the emulsifying capability, foaming, heat stability, solubility and decrease allergenicity more than solely protein. The basic principle behind these hydrophilic residues of polysaccharides will orient themselves to the neighboring water molecule while the hydrophobic residues of the denatured pro-

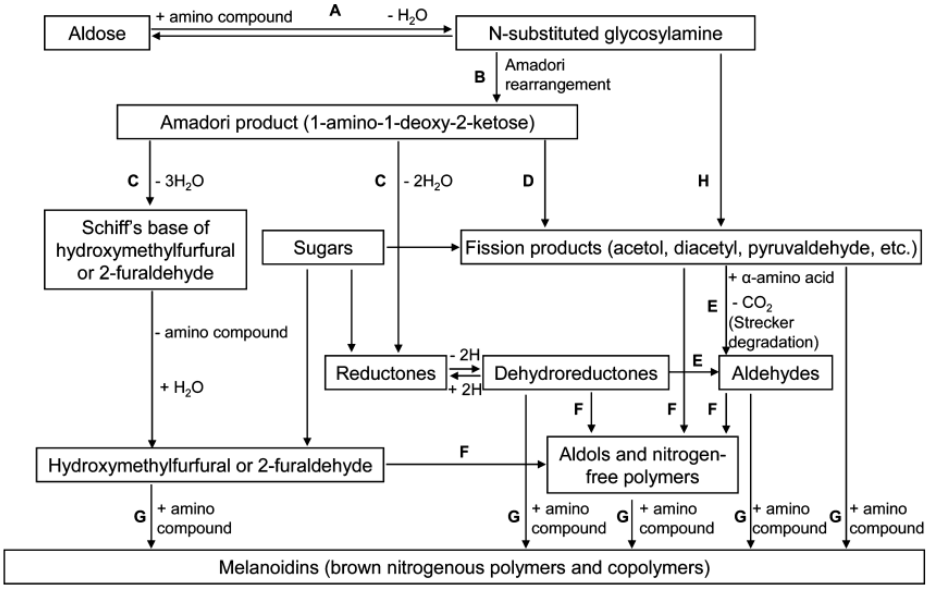

Figure 1.1 Diagram constructed by the John Hodge to make clear the Maillard reaction network [25].

teins can anchor to surface oil droplets. Additionally, the products have antimicrobial and antioxidative features, so they have been preferred in the cosmetics, tanning lotions and medicine [30]. In this thesis study the nanocapsules were produced in a heterophase system by using the BSA-Pectin conjugates produced by the Maillard reaction. There are various methods like heterophase polymerization, template-based approach involving layer by layer (LBL) assembly method, and self-assembly of the amphiphilic block copolymers, developed to produce nanocapsule in an organic solvent or in water [4]. In the LBL assembly method, colloidal particles that can create a polymer layer in the polymer solution are used as a template. Thanks to this method, multiple polymer layers can be deposited sequentially and produced nanocapsules can be good candidate for targeted delivery [31, 32]. Thanks to their useful mechanical features, controllable molecular weight, chemical variety and stability, amphiphilic polymers are beneficial tools. Especially, producing multifunctional nanoparticles for drug delivery and imaging applications, amphiphilic block-copolymers play an important role [32]. In polymer thin films, a range of well-ordered arrays of nanoparticles can be produced by the cooperative self-assembly of nanoparticles and block copolymers. In this method, controlling the interaction between nanoparticles and polymers direct the arrangement of

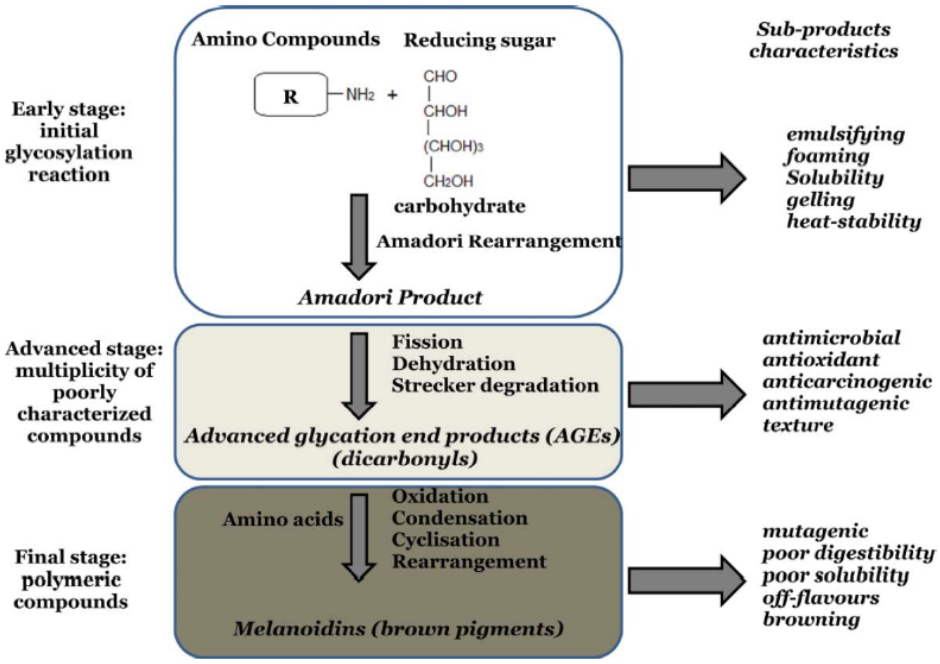

Figure 1.2 Simplified Maillard reaction stages with sub-products information [26].

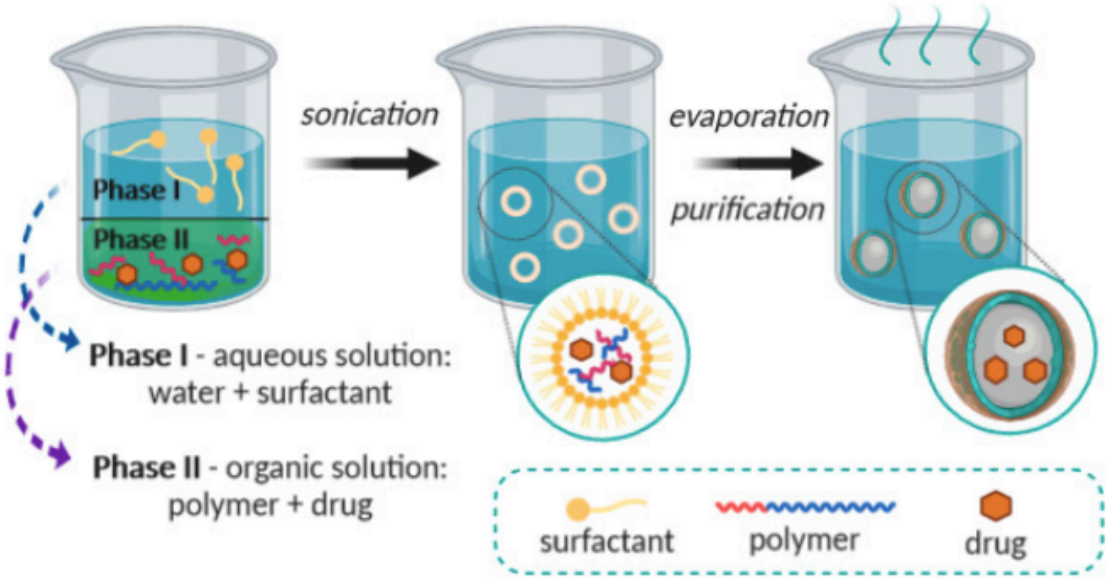

Figure 1.3 Schematic representation of the solvent evaporation method to produce nanoparticles from the preformed polymers [1].

the nanoparticles and nanoparticles are segregated into the interface between polymer domains. Thanks to the self-assembly process, block copolymer micelles encapsulating various types of nanoparticles in the hydrophobic core are produced [33].

To produce polymeric nanocapsules the other method is heterophase polymerization systems including (mini)emulsions and suspensions produced by the covalently linked polymers that cover the formed droplets [4]. In (mini)emulsion polymerization system, monomers are dispersed in an aqueous solution that includes surfactant and a water-soluble initiator starting the polymerization. Basically, in this system polymers are produced by heterogeneous nucleation which is the entrance of radicals into micelles, the homogeneous nucleation is the precipitation of growing oligomers in the aqueous phase and entry of radical in monomer droplets [34]. Polymeric nanocapsules are also produced by the preformed polymers, including solvent evaporation, spontaneous emulsification, salting out/emulsion diffusion and nonaqueous phase separation methods [35]. When polymer production is challenging in emulsions, the nanoparticle production is performed by the preformed polymers especially by using the solvent evaporation method [4]. In this method, the nanoparticles are produced by mixing of the water (aqueous, phase I) and water immiscible solvents like chloroform or

dichloromethane (organic, phase II). After the procedure, the residue of the organic solvent is evaporated [35].(Figure 1.3)

The main aim of this thesis study is producing totally biocompatible, biodegradable nanocontainers by using natural polymers BSA and Pectin. For this reason, the Bovine Serum Albumin and Pectin conjugates are produced via Maillard reaction. The produced conjugates are characterized by protein assay, SDS-PAGE and FT-IR methods to understand the Maillard reaction occurred effectively or not. By using the produced conjugates, the nanocontainers are produced by using oil in water miniemulsion technique. They are characterized by dynamic light scattering, zeta potential measurements and Scanning Transmission Electron Microscopy to determine the size, size distribution, zeta potential and morphology of the produced nanocontainers.

2. BACKGROUND

2.1 Bovine Serum Albumin (BSA)

The name albumin comes from a general term known as albumen which is an ancient German word used for the protein. The origin of the word is Latin, albus (white), means the color of the cooked egg's part surrounding the yolk. The most prominent plasma protein in the vertebrates's body is Albumin whose features have been known since the era of the Hippocrates [36]. Although, there are various source of the albumin (human, rat, horse, pig, snake...) the bovine serum albumin (BSA) used in this thesis study derived from the blood of the bovine. It is synthesized by the hepatocytes of the liver and pass the bloodstream and it works mainly on the coordinating the blood's colloidal osmotic pressure [36, 37].

2.1.1 Structure of the BSA

The BSA is a protein molecule having 66.4 kDa molecular mass with its 583 amino acids. Its single chain cross linked with eight disulfide bonds and a free thiol group to 17 cystine residues. Three structurally different (I, II, III) but homogeneous domains constitute the chain of the amino acid. Each of the domains having two internal domains which are A and B, have nine loops with the disulfide bonds and form a molecule shape like a heart. Seventy four percent of the BSA protein is -helical constitute its secondary structure, the other part of the molecule flexible, alternating and extending between the sub-domains [38]. The structure of the BSA tend to deteriorate between 42-50 °C, but it can be stable up to 40 °C [39]. Tryptophan 134 (Trp-134) located on the surface of the BSA in the domain IB and tryptophan 213 (Trp-213) located in the hydrophobic side of the domain IIA are two intrinsic fluorescence residues of the BSA. The intrinsic fluorescence of the BSA quenched when biomacromolecules interact with the BSA, so it is employed to understand in vivo biomacromolecule biodistribu-

tion and transportation by using fluorescence spectroscopy. [40]. The BSA is the one of the plasma proteins, includes methionine, isoleucine, tryptophan and glycine despite it has plenty of ionic amino acids like lysine, glutamic acids. The amino acid content generates the structural characteristic of the BSA. The total charge of the BSA comes from its ionized residues and increase its solubility. Each BSA molecule has 185 ions at neutral pH (7.0) [38].

2.1.2 Functional Properties of the BSA

When some molecules like hormones, xenobiotics, fatty acids and drugs go into the blood stream, their transportation and disposition can be possible by making a complex with the albumins of the serum. To maintain pH, osmotic pressure of the blood albumin plays an important role with its reversibly binding ability to other

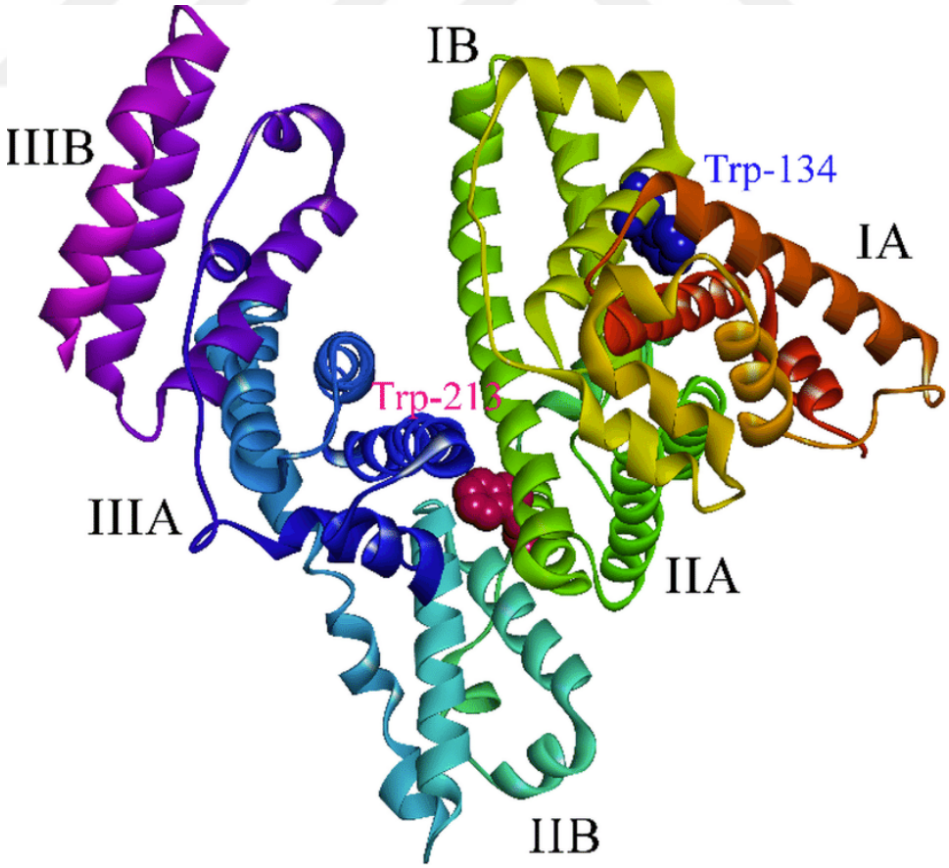

Figure 2.1 Schematic representation of the subdomains of the Bovine Serum Albumin and its tryptophan residues [40].

molecules [38]. The metabolism, efficacy and circulation of hydrophobic drugs are possible by the presence of the BSA in the blood because it increases the solubility of these drugs. On the other hand, in mammals the concentration of some active ions like Mg^2+, Ca^{2+} is controlled by the BSA [38]. Additionally, it has ability of transportation of the Zn^{2+} and Ca^{2+} in the blood plasma [41].

2.1.3 Biomedical Applications of the BSA

To deliver therapeutic agents and anticancer drugs the BSA is employed widely because of its biocompatible, biodegradable features and its lots of functional groups that can bind to drugs easily. Two different interaction methods that are non-covalent conjugation and covalent conjugation allow the interaction between the BSA and the drugs or therapeutic agents. Covalent conjugation is possible thanks to the carboxylic and amino groups on the BSA. On the other hand, the hydrophobic interaction, electrostatic interaction, encapsulation and chemical coordination are evaluated under non-covalent conjugation and allows the loading of the therapeutic agent and drugs by the help of the BSA. BSA is a nontoxic, biocompatible, and hydrophilic molecule. These features make it a good candidate for being surface modification agent of the nanomaterials. In addition to these, thiol, carboxyl and amino groups on the BSA allows the biomimetic synthesis of the metal oxide and metal nanoparticles used for the cancer imaging and image guided cancer therapy studies [39].

2.2 Pectin

The Greek word, meaning the firm and hard, *pectos* based on the gel forming ability of the pectin is etymon of the word 'pectin' [42]. The protopectin partaking in the middle lamellae and primary cell wall of the plants is the precursor form of the pectin. The protopectin is insoluble, but when it is turned to the pectin by ripening process, it becomes soluble [43, 44]. Dried citrus peel, apple pomace are the most common raw materials for the production of the pectin, although it is found nearly all

plants that it can be beneficial for the cell structure like sugar beet [42, 45].

2.2.1 Structure of the Pectin

Few hundred to thousand monomer units named as galacturonic acid linked with $\alpha-(1\rightarrow 4)$-glycosidic bond constitutes the backbone of the pectin which is a type of polymer. The pectin molecules have molecule weight averagely between 50 and 150 kDa. The neutral sugars like, L-rhamnose, D-galactose, D -xylose and L -arabinose inside the pectin makes relatively short side chains named as 'hairy regions' to the galacturonan backbone of the pectin [42]. However, $\alpha-(1\rightarrow 2)$ rhamnopyranose units (1,2-linked L –rhamnose) of the side chains of mannose, glucose, xylose and galactose substitute the backbone of the pectin molecule. In galacturonic acid units of the pectin, the methyl esterification occurs and this allows the formation of two different pectin types which are low methoxly and high methoxyl pectin. The characteristic feature of the low methoxly pectin is having less than 50% esterified galacturonic acid residues, on the other hand, having more than 50% esterified galacturonic acid residues means high methoxyl pectins [47]. The interaction of the pectin with other charged molecules like proteins, calcium is affected by the local electrostatic charge density of the pectin

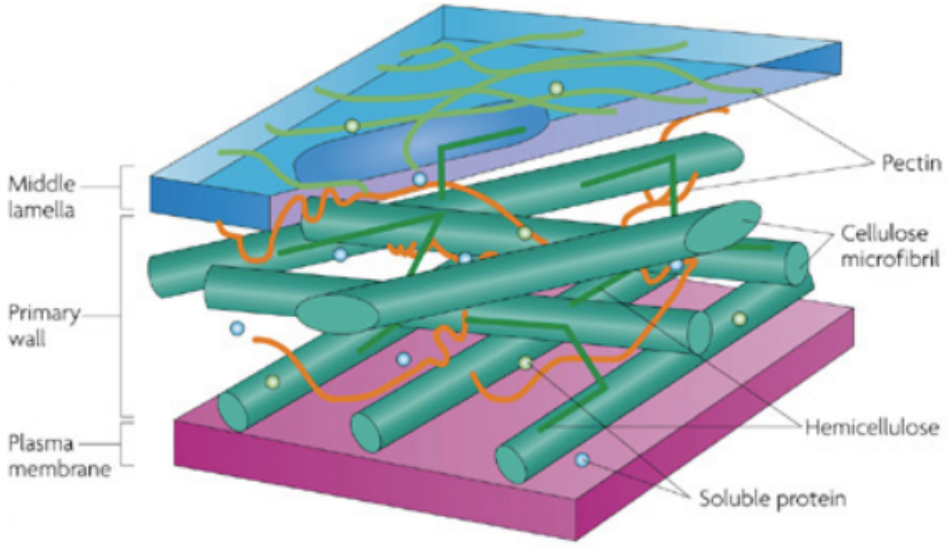

Figure 2.2 Cell wall of the plants surrounding and providing tensile strength to plant cell by its three layers which are the middle lamella, primary cell wall and the secondary cell wall (not in the figure) including hemicellulose, cellulose microfibrils, lignin, soluble protein and pectin [46].

determined by the distribution of esters [43]. For this reason, gel forming capacity of the low methoxyl pectins different from the high methoxyl pectins. They need calcium ions to form gel by constitute bridges cross linked pectin to hold the moisture. Also, the distribution and number of methyl-ester groups determine the solubilization rate of the pectin in the water. Additionally, the solubilization rate of the pectin affected by the temperature, ionic strength and pH of the dissolver. At pH level between the 2.5 and 4.5 the high methoxyl pectin is more stable, but as the pH level increase and go beyond the 4.5 the galacturonic acid chain depolymerize by -elimination. Low methoxly pectin are more stable at higher pH values because the depolymerization process needs to esterified carboxyl group stay near the glycosidic bond [42].

2.2.2 Functional Properties of the Pectin

The pectin reside in the middle lamellae and primary cell wall of the plants.It is a type of polysaccharide or in other words a heteropolysaccharide having important role in the regulation of the cell-to-cell adhesion, control the pore size of the cell wall

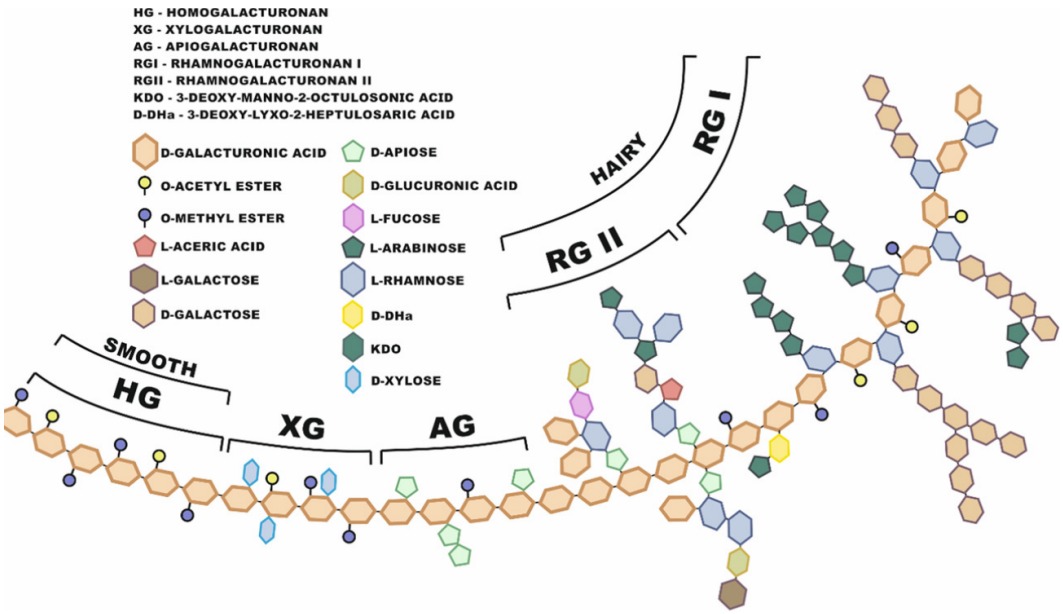

Figure 2.3 Schematic representation of pectin including the apiogalacturonan (AG), xylogalacturonan (XG), rhamnogalacturonan I (RG-I), rhamnogalacturonan II (RG-II), and homogalacturonan (HG) regions. The main structure constituting the 60% of total pectin is linear, the smooth pectin region is constituted by the moderately esterified homogalacturonan backbone. The many branches of RG I and RG II domains and a few AG and XG extends construct hairy regions. [44].

of the plants and eliciting the cellular responses [43, 44, 48].

2.2.3 Biomedical Applications of the Pectin

Pectin has the ability of binding water and increasing viscosity, so it is widely used in the food industry to increase gelling of jams in the confectionary industry, stabilize yoghurt and milk drinks in the dairy industry [45]. Also, it is working as a fat replacer in the production of emulsified meat products and ice creams. In addition to these applications, it has also applications in the medical field, especially in pharmaceutical industry because of its ability of decreasing blood fat, reducing the heart disease, soothing pain, inhibiting lipase activity. In addition to these, it also employed for the delivery of gene and drugs, tissue engineering and wound healing applications [49].

2.3 BSA-Pectin Maillard Reaction

The Maillard reaction also named as browning reaction occurs without using any external chemicals or enzyme. The characteristic brown color arises when the free amino groups of the protein react with the carbonyl groups of the sugar [50]. Guanido group and terminal amino of the arginine, $\epsilon - NH_2$ groups of the lysine, glutamic acid of the BSA react with the carbonyl groups of the pectin to form irreversible Maillard reaction products which is Amadori products, further they transform and constitute cross linked protein- oligosaccharide conjugate [38, 51]. The whole reaction process occurs spontaneously, but humidity, pH and temperature affect its quality [50]. Increasing in the pH influence the reaction positively because at low pH value the amino groups of protein protonated and they are not available for the reaction. Also, increasing in the temperature affects the Maillard reaction directly and positively, so the browning intensity value gets higher than the lower temperature [52].

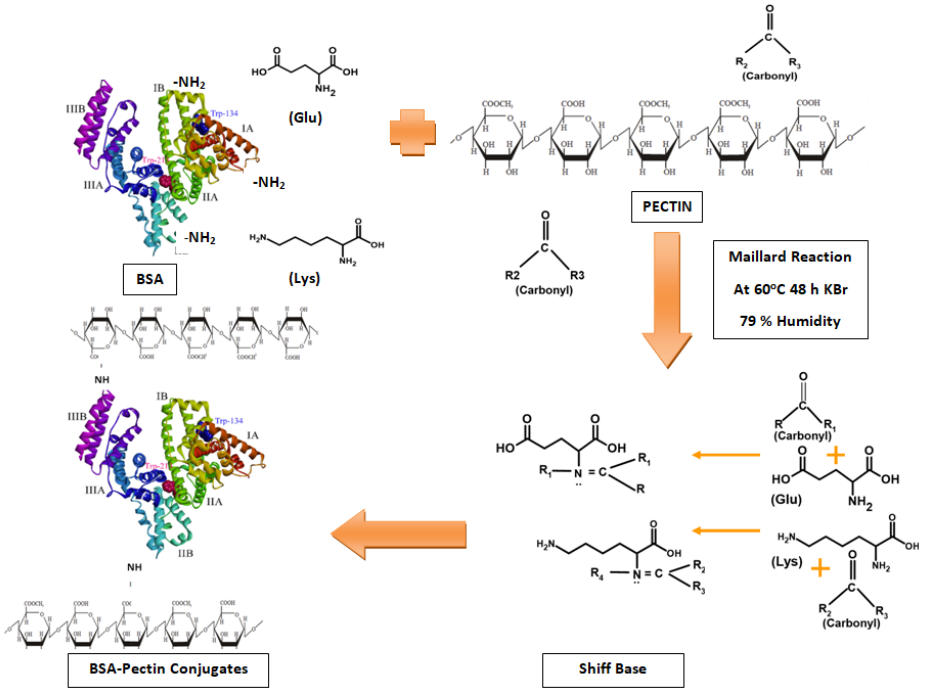

Figure 2.4 Shematic representation of the formation of the BSA-Pectin conjugates via Maillard reaction

3. MATERIALS AND METHODS

In this thesis study, BSA-Pectin conjugates were produced through the Maillard reaction and they were characterized by using protein assay, SDS-PAGE and FT-IR analysis. After these procedures, nanocontainers were produced by using the BSA-Pectin conjugates. Characterization of the nanocontainers was made by dynamic light scattering analysis, zeta potential measurements and scanning transmission electron microscopy images. Visual depiction of the whole procedure can be seen from the Figure 3.1.

3.1 Materials

Bovine Serum Albumin (BSA) (purity: $>$ 98 %), Olive Oil (highly refined, low acidity), Tween ® 20 (viscous liquid) were provided from Sigma-Aldrich. Pectin was bought from Alfasol.Potassium Bromide (KBr) (purity: $>$ 99 %), Sodium Hydroxide (NaOH) (purity: $>$ 97 %) were purchased from Acros Organics. Protein assay reagent; Pierce^{TM} 660 nm was acquired from Thermofisher. SDS-PAGE materials; 4X Bolt^{TM} LDS sample buffer (novex), 10X Bolt^{TM} reducing agent, 20X Bolt^{TM} MES SDS running buffer, Bolt^{TM} Bis-Tris running gels (10 %,10-well) , SimplyBlue^{TM} SafeStain (Coomassie Brilliant Blue) (invitrogen) were obtained from the ThermoFisher Scientific.

3.2 Preparation of the BSA-Pectin Conjugates via Maillard Reaction

BSA-Pectin conjugates were produced through the Maillard reaction by considering the studies of Chen H. et al., so BSA and Pectin mixtures were prepared with different m_{BSA}:m_{Pectin} weight ratios (1:7, 1:2, 2:1, 7:1) and the mixtures were dissolved

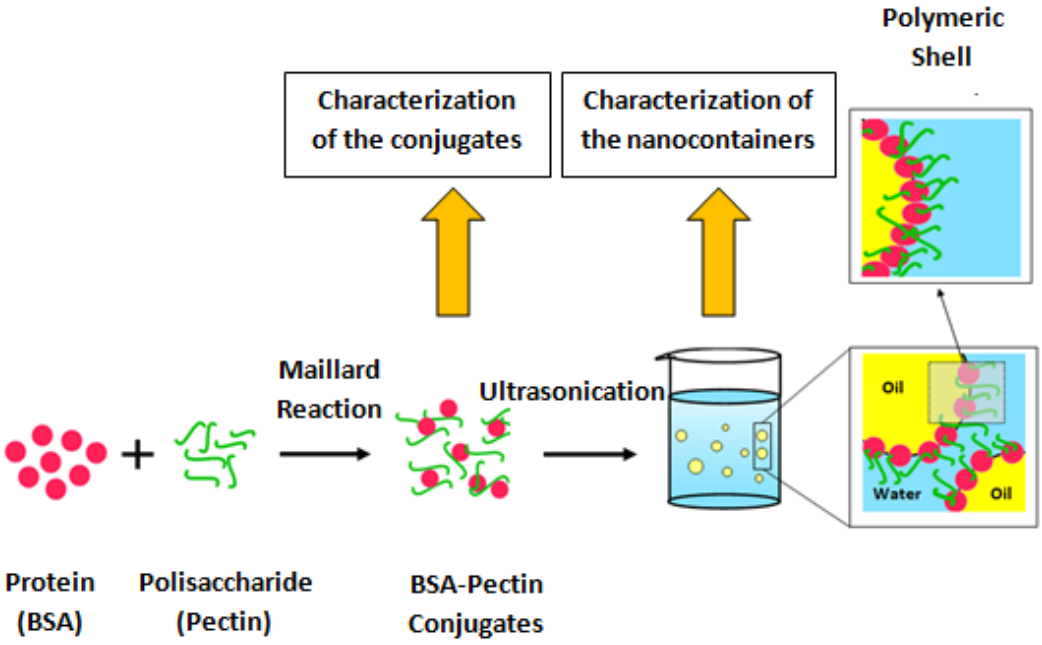

Figure 3.1 Schematic representation of the overall procedure in this thesis study.

in distilled water having 1.0 % (w/v) concentration [53]. However, other studies indicate that increasing the pH of the prepared mixtures positively affects the reaction because at low pH value the amino groups of the protein protonated and they are not available for the reaction [52]. For this reason, an additional solution including 2:1 BSA-Pectin weight ratio, having 1 % (w/v) concentration was prepared and its pH value was increased by using 0.1 M Sodium Hydroxide (NaOH), and prepared solutions were stirred overnight at ambient temperature. After these procedures, the solutions lyophilized by using Christ Alpha 1-4 freeze dryer. Finally, the lyophilized BSA-Pectin complexes placed into the desiccator including saturated KBr solution to supply 79 % humidity environment and incubated for 48 hours at 60°C [51, 53]. The produced conjugates were stored in the 4°C. The produced BSA-Pectin conjugates can be seen in the Figure 3.2.

3.3 Characterization of the BSA-Pectin Conjugates

BSA-Pectin conjugates were characterized by using Protein Assay to quantify the protein inside the conjugates, SDS-PAGE to evaluate the protein content of the

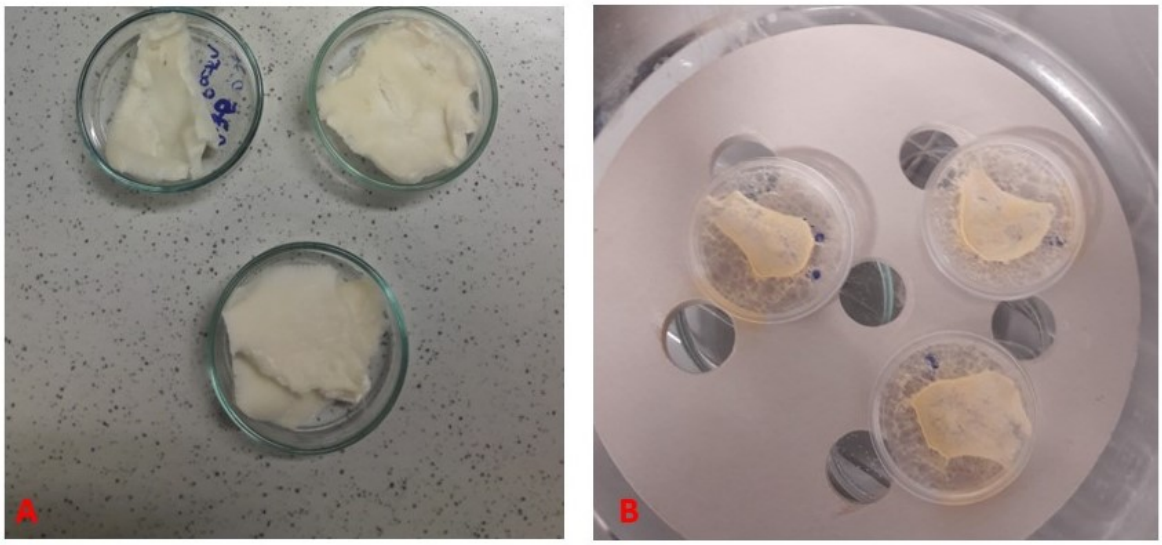

Figure 3.2 A) BSA-Pectin conjugates produced without any pH adjustment. B) BSA-Pectin conjugates produced with increased pH value.

conjugates and FT-IR Analysis to monitor binding between BSA and Pectin polymers.

3.3.1 Protein Assay

To determine protein concentration in a specimen, the analysis method should be highly sensitive, accurate, low cost and rapid [54]. There are various types of methods to quantify protein in a specimen, like favoring UV absorption of proteins directly, biuret methods based on protein-copper chelation and reduced copper detection, fluorescent dye methods based on protein-dye binding and detection of increase in fluorescence with regard to the bound dye. In addition to these methods, another way of determining the protein concentration in a specimen is colorimetric dye-based methods based on protein-dye binding and determination of the change in the color [55]. In this thesis study, Thermo Scientific Pierce 660 nm protein assay allowing colorimetric detection of the protein was used. It is ready to use, quick, compatible with many detergents, moderate for the protein variations and shows more linearity than the coomassie-based Bradford assay which is another colorimetric method for determination of protein. In this method, the protein amount inside the solutions is calculated by considering the calibration curve generated from the absorbance of the solutions

whose protein concentrations are known. [56]. For this reason, to produce calibration curve 10 mg BSA was dissolved in the 10 mL water and then 100 µL, 200 µL, 300 µL, 400 µL, 500 µL, 600 µL, 700 µL, 800 µL and 900 µL solutions were taken from the stock solution and they were completed to 1mL with water to get solutions including 100 µg/mL, 200 µg/mL, 300 µg/mL, 400 µg/mL, 500 µg/mL, 600 µg/mL, 700 µg/mL, 800 µg/mL, 900 µg/mL BSA concentrations. After that procedure, 10 μL samples were taken from these solutions putted into the microplate wells (96 well-plates), 150 µL protein assay reagent added on them, the plate was placed into the Bio-Rad iMark microplate reader, shaken for one minute and the absorbance values were measured at 655 nm. Lastly, the mean of the absorbance values was calculated and the calibration curve was created with the curve equation. The used protein assay reagent can determine the protein amount which is among 25 -2000 µg/mL. Therefore, to obtain protein in this range, 0.1 mg was weighted from each BSA-Pectin conjugate and dissolved in 1 mL water. After this procedure, 10 µL was taken from the prepared solutions putted into the microplate wells (96 well-plates), 150 µL protein assay reagent was added on them, the plate was placed into the microplate reader, shaken for one minute and absorbance values were measured at 655 nm. Lastly, the actual protein concentrations of the conjugates were calculated by using the equation of the produced calibration curve (See Appendix A.Figure A.1).

3.3.2 Sodium Dodecyl Sulfate-Polyacrylamide Gel Electrophoresis (SDS-PAGE)

To separate molecules according to their charges and sizes polyacrylamide gel electrophoresis is widely used. SDS is such a detergent that can denature the proteins' secondary structure and load them with negative charge while coating the proteins. In here, the negative charge amount of the proteins proportional to their size and length. This feature allows the estimation of the size of the proteins moved through SDS-PAGE system. In addition to this, sieving effect of gel matrix also provides the separation of the proteins in accordance with their indicated features [57, 58]. A typical SDS-PAGE gel consists of an upper stacking gel and lower resolving gel whose polyacrylamide

concentrations and pH values are different. The polyacrylamide concentration of the stacking gel located upper side is lower than the resolving gel stay in the bottom to provide both tight band and quick running before the proteins go to inside of the resolving gel. The concentration of the polyacrylamide can be tuned according to the size of the molecules in the sample. As the size of the protein molecules decrease the velocity of the molecules through the gel increase [57]. In this thesis study, Bolt^{TM} Bis-Tris Plus Mini Gels that can separate the proteins in 6-400 kDa size range were used. The gels have 10 wells and each well has maximum 60 µL sample capacity. To prepare samples for loading the wells, 0.1 mg BSA-Pectin conjugate dissolved in 1000 µL water and for each sample the microliter value including 2.5 µg protein was calculated. After, 2.5 µL LDS Sample Buffer (4X), 1.0 µL Reducing Agent (10X) and for each sample microliter value including 2.5 µg protein were taken and putted into the Eppendorf microtubes. Lastly, deionized water added in to each microtube so as to be total volume 10 µL [59]. Here, the reducing agent used for reducing the proteins, the sample buffer used to increase the activity of the reducing agent and also the Phenol Red and Coomassie G250 dyes inside of it allows tracking of the proteins while they are moving through the SDS-PAGE gel [60, 61]. After these procedures, the microtubes including the prepared solutions were heated in the heating block to allow the denaturation and make the proteins a straight band. The gel cassette was opened and placed into the Invitrogen Mini Gel Tank, the running buffer Bolt^{TM} MES SDS Running Buffer (20X) was diluted to 1X and 400 ml added into each tank to supply ion migration during the process [62, 63]. The ladder and only BSA including samples were injected into the first and second wells of the gel respectively, then the prepared samples of the different conjugates were placed into the wells. The system was connected to the power supply at 130 V (30 mA) and the procedure took around 45 minutes. Lastly, the gel was taken from the system and stained with Invitrogen SimplyBlue^{TM} SafeStain solution for overnight. 10 ml, 20% NaCI was added into this solution to increase its sensitivity [64]. After this procedure, the gel was washed with distilled water to make clear the bands of the proteins. Lastly, the image of gel was taken by using the Bio-Rad Doc XR scanner.

3.3.3 Fourier Transform-Infrared Spectroscopy (FT-IR) Analysis

FT-IR is a rapid method that can be an efficient tool for the analysis of bonding structure of the materials. In the instrument, a glowing black body source emits a beam of Infrared irradiation. While the produced beam passes through interferometer, destructive and constructive interferences occur. When the beam pass through the samples, the specific frequencies of the beam energy is absorbed by the samples according to features of the samples. The process is measured by a detector and a Fourier transformation computer software shows the spectrum obtained from the process [65]. To analyze mixtures, impurities, compositions of the materials and pure substances the FT-IR technique is used widely. Moreover, the technique is so beneficial to understand structural changes as a result of a chemical or biological processes [66]. For these reasons, in this thesis study the produced BSA-Pectin conjugates were analyzed by this technique to confirm the taking place of the Maillard reaction among the BSA and Pectin, analyze structural changes and bonding regions of them. The BSA, Pectin and the BSA-Pectin conjugates having 2:1 m_{BSA}:m_{Pectin} weight ratio (pH adjusted and non-pH adjusted) were analyzed by using Nicolet 380 FT-IR spectroscopy.

3.4 Nanocontainer Production

In this thesis study, the nanocontainers were produced by miniemulsion technique with preformed BSA-Pectin conjugates both using a surfactant and without using a surfactant. In here, the surfactant helps creating self-assembled clusters known as micelles of the molecules by interfering between two different phases [4, 67]. For this purpose, firstly to produce nanocontainers without using surfactant, 10 mg BSA-Pectin conjugate was weighted and dissolved into 10 ml water (as to be 1 mg/mL BSA-Pectin conjugate). After that, 100 mg olive oil was added into the mixture and mixed by using magnetic stirrer at 1000 rpm for 1 hour. The mixture was placed into the ultrasonicator (Branson-550 Sonifier) and ultrasonification was carried out at 90 % amplitude, for 4 minutes (15 seconds on and 5 seconds off) under ice cooling. On the other hand, other nanocontainers were produced by using surfactant to investigate the effects of

surfactant usage on the nanocontainers' features. To produce nanocontainers by using surfactant, 5 mg BSA-Pectin conjugate was weighted and dissolved into the 5 mL water. 5 mL Tween 20 (1 % V/V) solution mixed with 100 mg olive oil. The prepared two solutions were gathered in a vial and mixed by using magnetic stirrer at 1000 rpm for 1 hour. Lastly, the mixture was placed into the ultrasonicator (Branson-550 Sonifier) and ultrasonification was carried out at 90 % amplitude, for 4 minutes (15 seconds on and 5 seconds off) under ice cooling.

In addition to these, the nanocontainers were also synthesized by increasing the weight ratio of the conjugate from 1 mg/mL to 2 mg/mL and 3 mg/mL. The conjugate having 2:1 m_{BSA}:m_{Pectin} weight ratio produced by increasing pH (8.3) was preferred because its characterization results were efficient. The aim of this study was understanding the effect of increasing weight ratio of BSA-Pectin conjugates, on size, size distribution of the produced nanocontainers. For these reasons, to produce nanocontainers without surfactant 20 mg (2 mg/mL BSA-Pectin conjugate) and 30 mg (3 mg/mL BSA-Pectin conjugate) conjugates were dissolved in the 10 mL water respectively and same procedure indicated above was followed. On the other hand, to produce nanocontainers with surfactant, 10 mg (2 mg/mL BSA-Pectin conjugate) and 15 mg (3 mg/mL BSA-Pectin conjugate) conjugates were dissolved in 5 mL water, mixed with 5 mL Tween 20 (1 % V/V) solution and same procedure indicated above was followed.

Additionally, to investigate the purification effect on size and size distribution of the produced nanocontainers, centrifugation and syringe filtration processes were applied. The nanocontainer produced with 2:1 m_{BSA}:m_{Pectin} weight ratio at increased pH was chosen by considering its favorable characterization results. For these reasons, the centrifugation process was performed three times at 20000 g and 25°C for one hour, the residual part taken and 1 mL water added. Syringe filtration was made by using 0.45 µm cellulose mixed ester syringe filter [68, 69].

3.5 Characterization of the Nanocontainers

The produced nanocontainers were characterized by solid content measurements to determine the amount of the solid part of the produced samples, DLS measurement

to understand the nanocontainers' size and poly dispersity, Zeta potential measurement to understand their zeta potential, STEM imaging to understand their morphology.

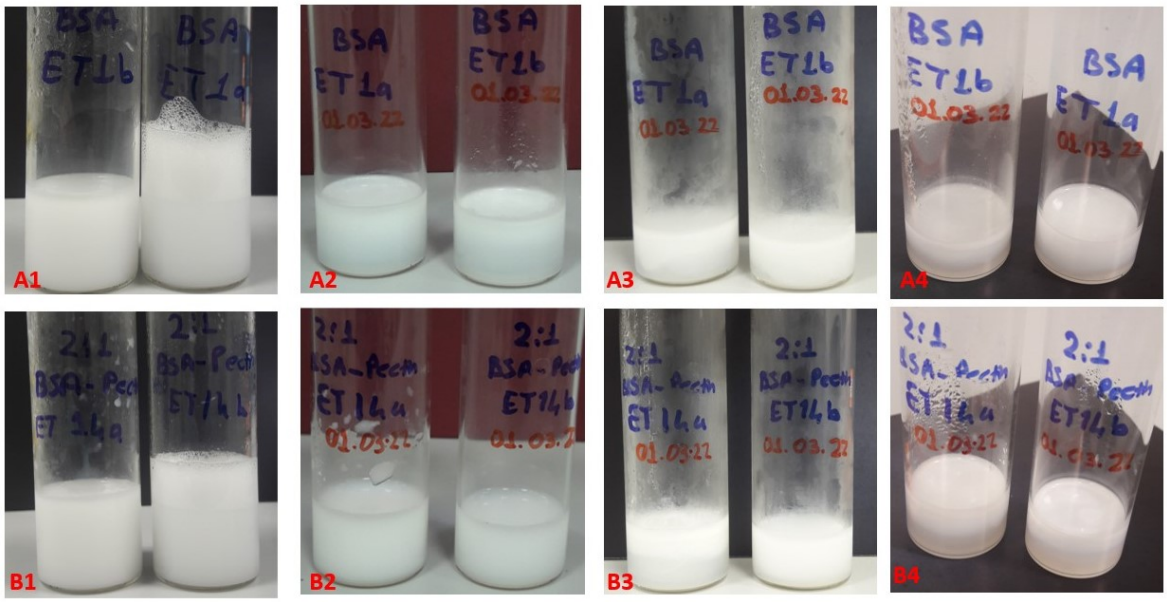

Figure 3.3 A1) The initial dispersions including nanocontainers produced with solely BSA produced with surfactant and without using surfactant. A2) Dispersions after one month storage period. A3) Dispersions after two month storage period. A4) Dispersions after three month storage period. B1) The initial dispersions including nanocontainers produced with BSA-Pecin conjugate having 2:1 m_{BSA}:m_{Pectin} weight ratio produced with surfactant and without using surfactant. B2) Dispersions after one month storage period. B3) Dispersions after two month storage period. B4) Dispersions after three month storage period.

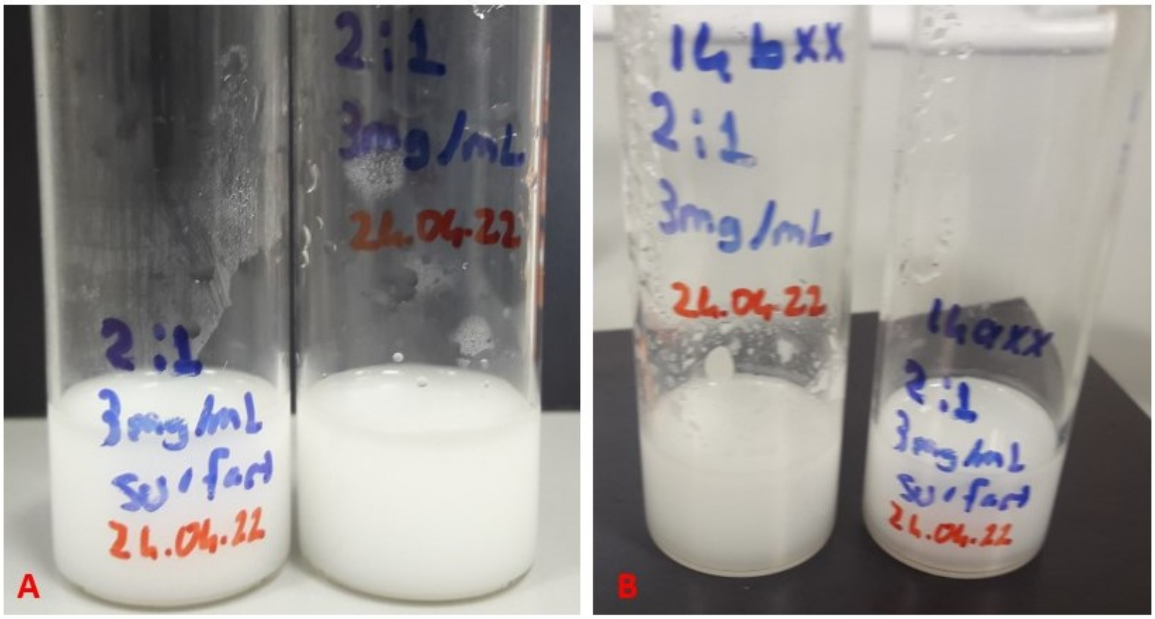

Figure 3.4 A) The initial dispersions including the nanocontainers produced with BSA-Pectin conjugate having 2:1 m_{BSA}:m_{Pectin} weight ratio and prepared at increased pH value by using surfactant and without surfactant. B) Dispersions after one month storage period.

3.5.1 Solid Content Measurement

The amount of the solid parts of the produced emulsions including nanocontainers were measured by firstly weighting the Eppendorf microtube and 100 µL emulsion. The Eppendorf tubes including the emulsions were placed into the freeze dryer, weight of the remaining solid part was calculated by subtracting the weight of the tube. This procedure was repeated three times for each emulsion.

3.5.2 Dynamic Light Scattering (DLS) Measurement

The Dynamic Light Scattering is a technique based on focusing a laser on dispersed particles and analyzing the scattered light [70]. Thanks to this technique, the diffusion coefficient, polydispersity and hydrodynamic radii of the particles in a dispersion are determined. The results of the measurements are directly related with the viscosity of the solvent inside the solution, size of the particle and temperature. In this technique the exact temperature of the solution is highly important because it affects the solvent viscosity [71]. For these reasons, in this thesis study, the size and polydispersity of the produced nanocontainers were measured by using DLS. The measurements were done by using Malvern Zetasizer Nano ZS at 25 ^{o}C , by considering the water (refractive index 1.330) as a dispersant in glass cuvette having square aperture. For each sample the measurement was done three times.

3.5.3 Zeta Potential Measurement

In a colloidal system the electrokinetic potential is represented by zeta potential [72]. The concentration of the opposite charge near the nanoparticle surface allows the demonstration of the nanoparticle's net surface charge. The zeta potential indicates the difference in potential between the bulk fluid (dispersant) and the oppositely charged fluid layer around the nanoparticle surface. The stability of the particle can be estimated from the magnitude of the zeta potential. Increase in the electrostatic re-

pulsion observed as higher magnitude of potential and that means higher stability [73]. For this reason, emulsions with low zeta potential (positive or negative) tend to coagulate while the emulsions with high zeta potential are more stable in case of electrostatic stabilization. There are various factors affects the zeta potential, but the main ones are medium pH, temperature, ionic strength and concentration of external additions to the system [72]. In this thesis study, the zeta potential measurements were done by using Malvern Zetasizer Nano ZS at 25 ^{o}C , by considering the water (refractive index 1.330) as a dispersant in clear disposable zeta cell.

3.5.4 Scanning Transmission Electron Microscopy (STEM) Imaging

In engineering and material sciences to analyze structures at atomic scale the scanning transmission electron microscopy (STEM) is a commonly used, versatile instrument [74]. Basic logic behind its working principle is finely focusing a beam of electrons trough a specimen and scanning across the specimen [75]. Image of the specimen is produced from the detection of scattered and transmitted electrons by using placed detectors as a function of position of the raster. The control of the contrast feature of the image and its formation can be controlled by making changes in the geometry of the detector [74]. While the other electron microscopes TEM produce image from the transmission of the electrons passing through the sample and the SEM produce image from the detection of the knocked-off and reflected electrons from the sample. Therefore, while the TEM gives information about the inner structure of the specimen, the SEM shows the surface feature of the specimen [76]. Simultaneously usage of the many detectors is an advantage of the STEM system. Therefore, both high angle, low angle and from the axis scattered electrons can be recorded. Simultaneously recording the whole image is an advantage for the TEM system, but being complex of the simple structures' image is a disadvantage of this system. In this system, thickness of the sample and focus are complicated functions specifying the image contrast, so determining best view of the investigated sample is difficult. Contrary to this, in STEM system in addition to many signals gives information about the image of the investigated structure, there is also Z-contrast image produced from the collection of the

scattered-out electrons at high angles with the detector named as high-angle annular dark field, making simpler understanding the structure of the sample. In this thesis study, the produced nanocontainers' morphology was observed by using the Thermo Scientific Quattro S system [77].

4. RESULTS AND DISCUSSION

4.1 Characterization Results of the BSA-Pectin Conjugates

The BSA-Pectin conjugates produced via Maillard reaction were characterized by using the following methods;

1. Protein Assay
2. Sodium Dodecyl Sulfate-Polyacrylamide Gel Electrophoresis (SDS-PAGE)
3. Fourier Transform-Infrared Spectroscopy (FT-IR)

The results of these characterization techniques are given below.

4.1.1 Protein Assay

In this thesis study, the quantification of the protein in the produced BSA-Pectin conjugates was done with protein assay method. The produced conjugates having different weight ratios which are 1:7, 1:2, 2:1 and 7:1 represents m_{BSA}:m_{Pectin} ratios. The Table 4.1 shows the results of the protein assay studies. In here, expected protein amount was calculated by considering protein amount in the conjugate dissolved in the water. The protein amount was determined by considering the equation of the trend line of the generated calibration curve and absorbance value of each sample. The efficiency of the conjugate having 1:7 m_{BSA}:m_{Pectin} weight ratio was calculated 92.31 %, the efficiency of the conjugate having 1:2 m_{BSA}:m_{Pectin} weight ratio was calculated 90.90 %, the efficiency of the conjugate having 2:1 m_{BSA}:m_{Pectin} weight ratio was calculated 94.12 %, and the efficiency of the conjugate having 7:1 m_{BSA}:m_{Pectin} weight ratio was calculated 66.28 %. The results of the protein assay study show that there is consistence between the expected and calculated protein amount of each conjugate.

Table 4.1 Results of the protein assay studies on the produced BSA-Pectin Conjugates

$\mathbf{m_{BSA}}$:$\mathbf{m_{Pectin}}$	**Absorbance with STD**	**Protein Amount (µg/mL)**
1:7	0.019±0.00294	120±15
1:2	0.118±0.02475	300±14
2:1	0.024±0.00740	640±21
7:1	0.015±0.02358	570±21

Table 4.2 Protein Assay results of the BSA-Pectin conjugates (m_{BSA}:m_{Pectin} weight ratio is 2:1) prepared without making any pH adjustment and prepared by increased pH value.

$\mathbf{m_{BSA}}$:$\mathbf{m_{Pectin}}$	**pH of the Conjugate Preparation Mixture**	**Absorbance with STD**	**Protein Amount (µg/mL)**
2:1	5.2	0.024±0.0074	640±21
2:1	8.3	0.038±0.0303	720±20

However, the most efficient was the conjugate having 2:1 m_{BSA}:m_{Pectin} weight ratio. For this reason, it can be assumed that the process used to produce the conjugates is suitable for the preserving used protein. Therefore, its characteristic features can be utilized in the nanocontainer production process.

Although the results of the protein assay studies on conjugates prepared without pH adjustment were satisfying, other researches indicate that increasing the pH of the prepared mixtures positively affects the Maillard reaction because at low pH value the amino groups of the protein protonated and they are not available for the reaction [52]. Therefore, it can be stated that pH adjustment allows the covalent binding among the BSA and Pectin, but without pH adjustment physical interactions may be more dominant among them [78]. For these reasons, the conjugate having 2:1 m_{BSA}:m_{Pectin}

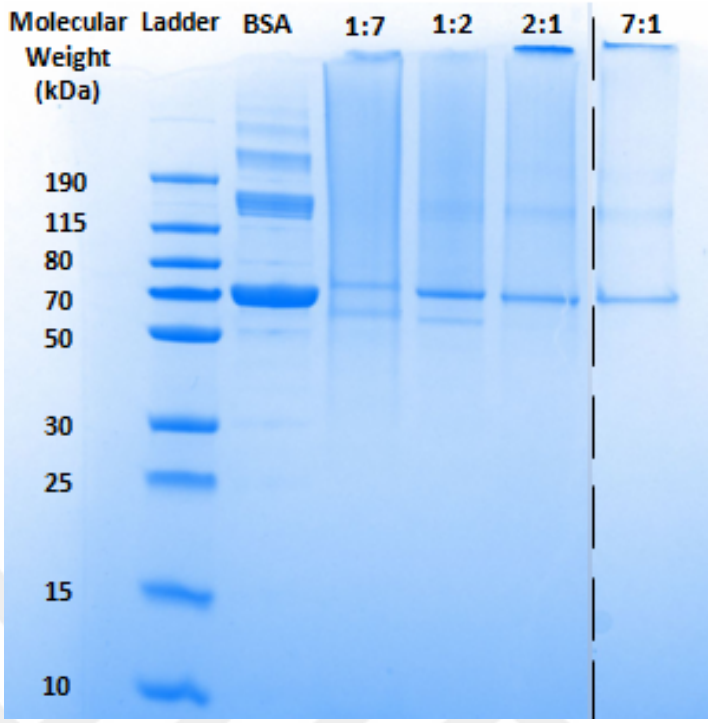

Figure 4.1 Image of the SDS-PAGE gel shows the weight ratio distributions of the reference Ladder, only BSA and BSA-Pectin conjugates having 1:7, 1:2, 2:1,7:1 m_{BSA}:m_{Pectin} weight ratios respectively.

weight was chosen to study the effect of pH adjustment on the conjugation process. Therefore, an additional protein assay study was performed on the conjugate produced by increasing the pH. The Table 4.2 shows result of this study. According to the results of the study performed only for the BSA-Pectin conjugate including 2:1 m_{BSA}:m_{Pectin} weight ratio, there are no big differences between the expected and calculated protein amount of the conjugates prepared by pH adjustment and without pH adjustment. The conclusion of this study is increasing in the pH does not affect negatively the used protein in the process. The results are consistent with literature as BSA molecules are considered stable at pH 7 and tend to be denaturated at low pH values [79–81].

4.1.2 Sodium Dodecyl Sulfate-Polyacrylamide Gel Electrophoresis (SDS-PAGE)

The SDS-PAGE study was performed for the conjugates having different BSA-Pectin weight ratios (m_{BSA}:m_{Pectin}). The aim was understanding the effectiveness of the conjugation when different weight ratios of the BSA and Pectin are used. The

analysis was based on the comparison between the reference Ladder, BSA and different BSA-Pectin conjugates. The Figure 4.1 shows the molecular weight distribution of Ladder, BSA and the conjugates having m_{BSA}:m_{Pectin} weight ratios 1:7, 1:2, 2:1, 7:1 respectively. When the results of the study analyzed, it can be clearly seen that BSA shows a significant band around 70 kDa. When the molecular weight of the BSA which is 66 kDa considered, the significant band is meaningful and consistent. The BSA also shows band pattern at higher molecular weights that can be arise from the aggregation of BSA molecules during the sample preparation procedure of the SDS-PAGE. On the other hand, the conjugates show disorderly band pattern nearly in all different weight ratios. Especially, the distributions around the higher molecular weights indicate that the conjugations were occurred.

4.1.3 Fourier Transform- Infrared Spectroscopy (FT-IR) Analysis

In this study, the FT-IR analysis was performed on the solely BSA, solely Pectin and the BSA-Pectin conjugate having 2:1 m_{BSA}:m_{Pectin} weight ratio to understand the binding between the BSA and Pectin. In addition to this, the FT-IR analysis was done for the conjugate having 2:1 m_{BSA}:m_{Pectin} weight ratio prepared with pH adjustment to evaluate the effect of the pH adjustment on the conjugation of the BSA and Pectin. The basic logic behind this analyze is making comparison between the FT-IR results of the solely BSA, the solely Pectin and the conjugates. When the FT-IR spectrum of these materials analyzed for the conjugates both prepared with pH adjustment and without making any pH adjustment, at the spectra the wavenumbers around 3270 cm^{-1}, 2930 cm^{-1}, 2332 cm^{-1} and 1621 cm^{-1} peaks were seen in the conjugate prepared without pH adjustment. The difference of the conjugate prepared with the pH adjustment was observed at 1651 cm^{-1} peaks. According to the theoretical searches, the FT-IR spectra the higher wavenumbers among the 2500-4000 cm^{-1} represents the single bond region and the peaks among the 3500- 3100 cm^{-1} represents primary and secondary amides stretch. Further, for this region the peaks can represent O-H stretches because there can be an overlap for the N-H and O-H groups in this region. Additionally, the peaks around the 3000 cm^{-1} represents the C-H stretches. Although, the peaks

around the 2000-2500 cm^{-1} are evaluated under the triple bond region, but for the 2332 cm^{-1} the theoretical approaches indicate N-H stretches or amino related components. And the peak at 1621 cm-1 indicates the N-H bending in primary amides, while the peak at 1651 cm^{-1} indicates primary amide absorption or C=O stretching in primary amides [65,82,83]. According to these FT-IR spectra results, it is assumed that the pH adjustment does not cause a big difference in terms of binding regions among the BSA and Pectin when producing them by Maillard reaction. Additionally, these results show the binding between amino groups of the protein and carbonyl groups of the polysaccharide was occurred successfully.

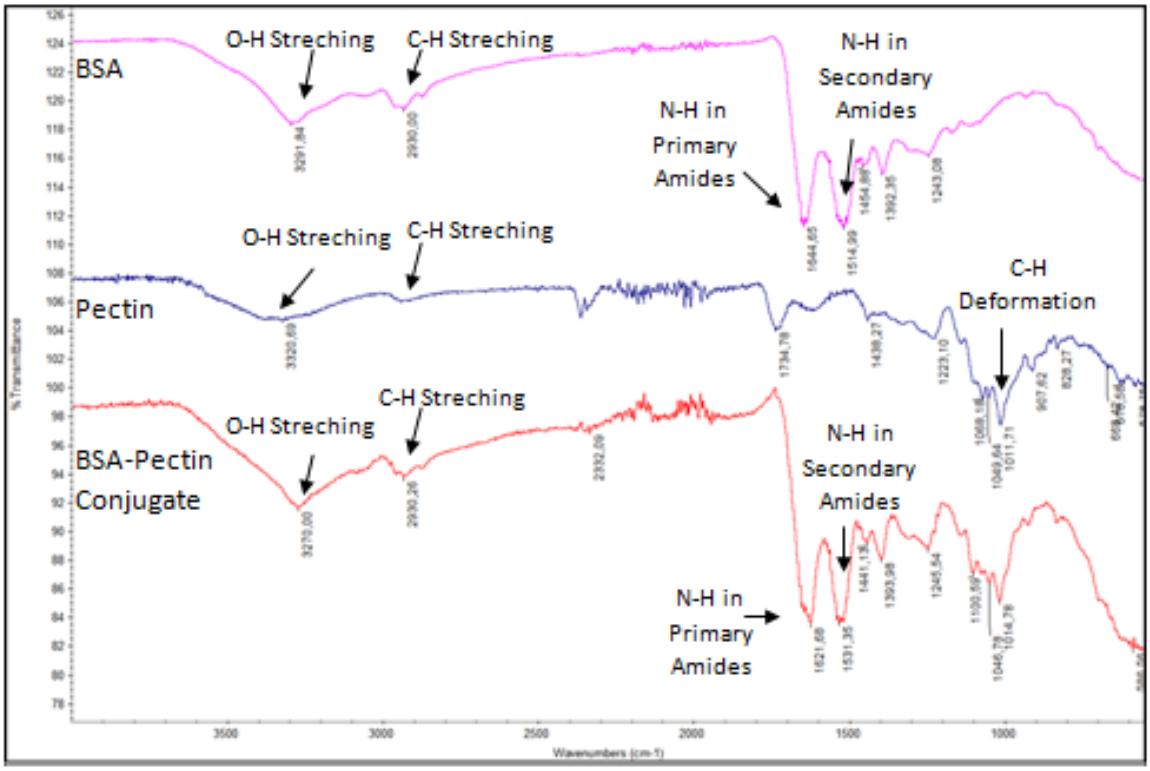

Figure 4.2 The FT-IR Analysis of the solely BSA (pink curve), solely Pectin (blue curve) and the BSA-Pectin conjugate with 2:1 m_{BSA}:m_{Pectin} weight ratio prepared without making any pH adjustment (red curve).

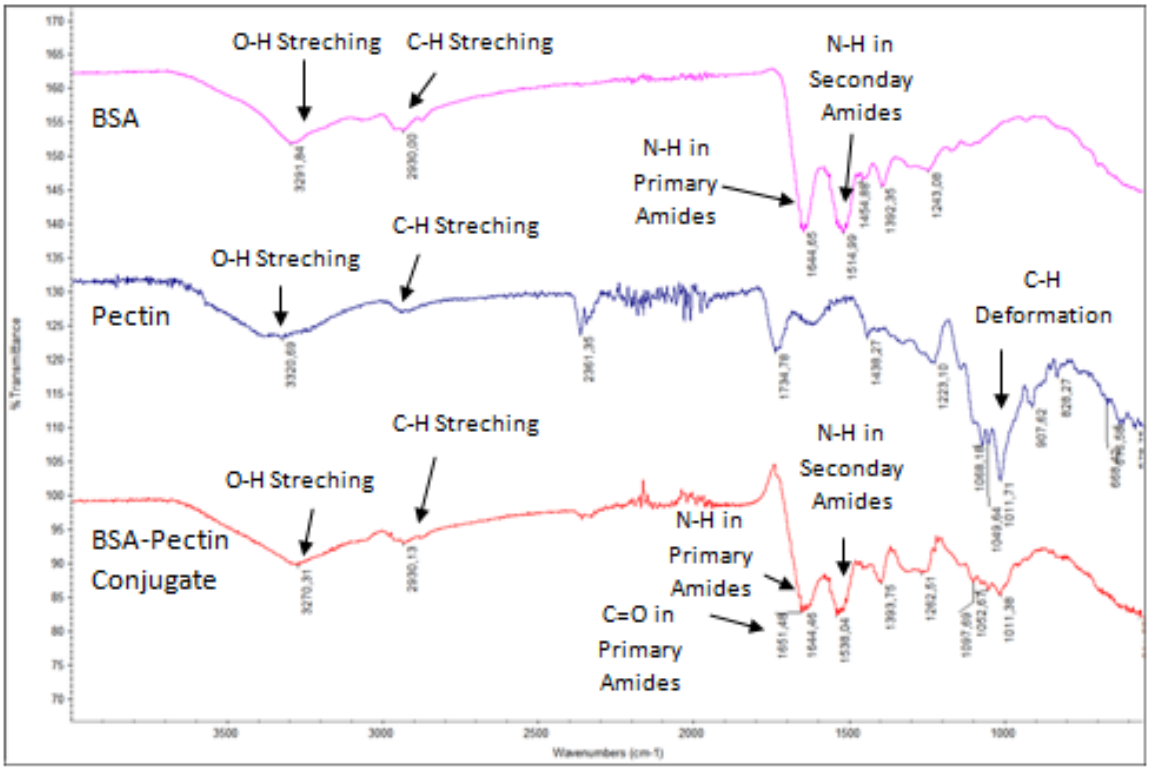

Figure 4.3 The FT-IR Analysis of the solely BSA (pink curve), solely Pectin (blue curve) and the BSA-Pectin conjugate with 2:1 (m_{BSA}:m_{Pectin}) weight ratio prepared by making pH adjustment (red curve).

4.2 Characterization Results of the Nanocontainers

The produced nanocontainers were charecterized by using three different methods as follows;

1. Dynamic Light Scattering (DLS) Measurement
2. Zeta Potential Measurement
3. Scanning Transmission Electron Microscopy (STEM) Imaging

The results of these measurements were given below.

4.2.1 Dynamic Light Scattering (DLS) Measurements

The dynamic light scattering measurements were to understand the size and the polydispersity index of of the produced nanocontainers. The size and polydispersity index of the produced nanocontainers were investigated in terms of four different variations which are given below.

4.2.1.1 Effect of the BSA-Pectin Weight Ratio and Surfactant Usage

The first dynamic light scattering measurements were made on the nanocontainers produced by using the BSA-Pectin conjugates having different m_{BSA}:m_{Pectin} weight ratios (1:7, 1:2, 2:1, 7:1). The aim was to understand the effect of the different BSA-Pectin weight ratios on the size of the produced nanocontainers and polydispersity index of the sample. Additional measurements were performed on the nanocontainers produced by using solely BSA to compare emulsifying feature of the BSA with the conjugates. The measurements were also carried out to nanocontainers produced by using surfactant to investigate the effect of surfactant usage on the nanocontainers' features. In addition to all these, the solid contents of the produced samples were analyzed to understand the solid part of the produced samples. The size, polydispersity index measurement results and solid contents of the produced nanocontainers were given in the Table 4.3. When the results are reviewed, it can be seen that the size of the nanocontainers decreases as quantity of the BSA increases in case of non-using surfactant. This result is consistent with the literature indicates that complexation can suppress the micellization ability of the protein [84]. The reason behind this result is the amphiphilic feature of the BSA. On the other hand, the surfactant usage also effective to decrease the size of the nanocontainer. When the feature of the surfactant is considered, the result is also acceptable. (Figure 4.4). The results also show that the changing in the weight ratio does not effective to decrease the PDI value. It can be concluded from the results that the variations in the binding between the BSA and Pectin molecules give rise to variations in the size distributions of the nanocontainers or increase the PDI value.

Table 4.3 DLS measurement results of the produced nanocontainers.

m_{BSA}:m_{Pectin}	pH Adjustment of the Used Conjugate	Surfactant Usage	Mean of Z-Average (d.nm) with STD	PDI Value with STD	Solid Contents (wt%)
Solely BSA	No	+	195.3±3.342	0.418±0.014	1.60
Solely BSA	No	-	268.0±5.183	0.437±0.022	0.91
1:7	No	+	208.8±2.762	0.431±0.027	1.00
1:7	No	-	1281.0±9.644	0.488±0.031	1.06
1:2	No	+	236.6±4.402	0.433±0.015	0.87
1:2	No	-	694.1±4.099	0.317±0.020	0.87
2:1	No	+	195.4±1.000	0.394±0.004	1.40
2:1	No	-	462.1±13.36	0.572±0.017	1.17
7:1	No	+	198.1±4.053	0.400±0.018	0.94
7:1	No	-	391.9±1.229	0.420±0.031	1.25

4.2.1.2 Effect of the pH Adjustment

The other DLS measurements were performed on the nanocontainers produced with the conjugates having 2:1 m_{BSA}:m_{Pectin} weight ratio at increased pH value. (pH

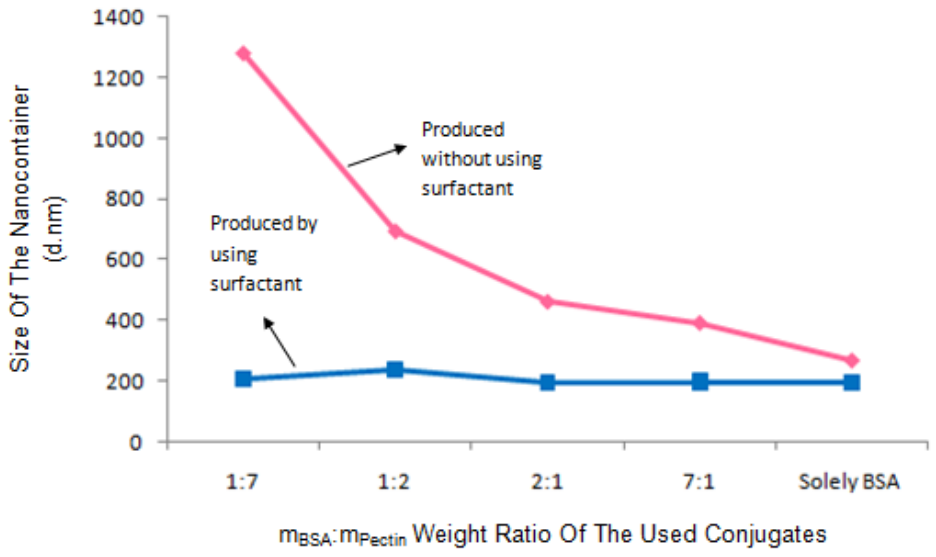

Figure 4.4 The size of the nanocontainer vs m_{BSA}:m_{Pectin} weight ratio of the used conjugate to produce the nanocontainer.

Table 4.4 The DLS measurement results of the nanocontainers produced with the conjugates, having 2:1 m_{BSA}:m_{Pectin} weight ratio prepared by both pH adjustment and without pH adjustment.

m_{BSA}:m_{Pectin}	pH of the Conjugate Preparation Mixture	Surfactant Usage	Mean of Z-Average (d.nm) with STD	PDI Value with STD	Solid Contents (% wt)
2:1	5.2	+	195.4±1.000	0.394±0.004	1.40
2:1	5.2	-	462.1±13.36	0.572±0.017	1.17
2:1	8.3	+	186.6±4.565	0.403±0.015	1.20
2:1	8.3	-	281.7±7.445	0.469±0.019	0.60

8.3). The main aim was here, to examine the theoretical approaches indicate that increasing the pH of the prepared mixtures positively affects the Maillard reaction because at low pH value the amino groups of the protein protonated and they are not available for the reaction [52]. If the conjugates produced precisely by Maillard reaction, they can show better emulsification property [85]. Therefore, the comparison made by considering the nanocontainers produced with both pH 8.3 adjusted and pH 5.2 adjusted conjugates. The DLS measurement results of these nanocontainers can be seen from Table 4.4. When the results are examined, it can be clearly seen that the size of the nanocontainers produced with the conjugates prepared without pH adjustment higher than the size of the nanocontainers produced with pH adjustment. Thus, it can be concluded that increase in the pH of the conjugate preparation mixture improves the quality of the Maillard reaction as indicated in the literature. Therefore, the nanocontainers produced with the conjugates prepared by increase in the pH have better emulsification property than the others. On the other hand, adjustment of the pH does not look effective to decrease the PDI value of the nanocontainers. It can be concluded from the results that there are still some variations in the bonding of the molecules and these give rise to variations in the size of the nanocontainers or increase in the PDI value.

4.2.1.3 Effect of the BSA-Pectin Conjugate Concentration

The DLS measurements were also performed on the nanocontainers produced with higher concentration (2 mg/ml, 3mg/ml) of the conjugates prepared with 2:1 m_{BSA}:m_{Pectin} weight ratio at pH 8.3. The measurement results can be seen from the Table 4.5. According to these results, there is no direct effect of the conjugate concentration on the size and size distribution of the nanocontainers. However, there are other studies argue that the change in the conjugate concentration directly affect the size of the nanocontainers [86]. This can be originated from the reaching the maximum capacity by increasing the conjugate amount in the continuous phase.

Table 4.5 The DLS and solid content measurement results of the nanocontainers prepared by using the solution including 1mg/ml, 2mg /ml and 3 mg/ml BSA-Pectin conjugates having 2:1 m_{BSA}:m_{Pectin} weight ratio prepared with increased pH value (pH 8.3).

m_{BSA}:m_{Pectin}	**Conjugate Amount (mg/ml)**	**Surfactant Usage**	**Mean of Z-Average (d.nm) with STD**	**PDI Value with STD**	**Solid Contents (% wt)**
2:1	1	+	186.6±4.565	0.403±0.015	1.20
2:1	1	-	281.7±7.445	0.469±0.019	0.60
2:1	2	+	176.9±3.465	0.357±0.005	1.57
2:1	2	-	372.5±20.51	0.525±0.039	1.14
2:1	3	+	184.9±3.041	0.380±0.036	1.16
2:1	3	-	266.0±3.041	0.354±0.071	1.34

4.2.1.4 Effect of the Purification

The other DLS measurements were performed on the nanocontainers processed with the purifications. The nanocontainers produced from the conjugates prepared with 2:1 m_{BSA}:m_{Pectin} weight ratio with pH adjustment were preferred for the centrifugation process to decrease the size and polydispersity. The results can be seen from the Table 4.6. Although the centrifugation process was effectively used for the purification in other studies, the results in the table show that there are increase in the size and polydispersity of the nanocontainers [68]. This can be originated from the density of the used materials, BSA and olive oil are lower than the density of the water, so the centrifugation was not effective to select smaller size of the nanocontainers. The other purification process which is syringe filtration was applied on the nanocontainers having same weight ratio. For this process, the smaller nanocontainers that can pass the filter were selected, so the syringe filtration was applied on the nanocontainers prepared by surfactant. The results of this study can be seen from Table 4.7. The results show that the syringe filtration is effective to decrease the size and polydispersity index of the nanocontainers.

Table 4.6 The DLS and solid content measurement results after the centrifugation process.

m_{BSA}:m_{Pectin}	pH of the Conjugate Preparation Mixture	Surfactant Usage	Mean of Z-Average (d.nm) with STD	PDI Value with STD	Solid Contents (% wt)
2:1	8.3	+	564.1±8.266	0.473±0.016	0.20
2:1	8.3	-	399.1±45.45	0.475±0.037	0.20

Table 4.7 The DLS and solid content measurement results after the syringe filtration process.

m_{BSA}:m_{Pectin}	pH of the Conjugate Preparation Mixture	Surfactant Usage	Mean of Z-Average (d.nm) with STD	PDI Value with STD	Solid Contents (% wt)
2:1	5.2	+	155.4±0.854	0.274±0.006	1.00
2:1	8.3	+	148.7±1.457	0.237±0.002	1.40

Table 4.8 Zeta potential measurement results

m_{BSA}:m_{Pectin}	pH of the Conjugate Preparation Mixture	Surfactant Usage	Zeta Potential Measurement (mV)
2:1	5.2	+	-37.7±0.985
2:1	5.2	-	-59.1±0.850
2:1	8.3	+	-43.4±0.603
2:1	8.3	-	-57.2±0.874

4.2.2 Zeta Potential Measurements

To understand the electro kinetic feature of the system the zeta potential measurements were performed on the samples including the nanocontainers produced by both the BSA-Pectin conjugate having 2:1 m_{BSA}:m_{Pectin} weight ratio produced without pH adjustment and with pH adjustment. The Table 4.8 shows the results of the measurements. From the results, it can be clearly seen that using nonionic surfactant decrease the zeta potential values as expected although all nanocontainers are still highly negatively charged.

4.2.3 Scanning Transmission Electron Microscopy (STEM) Imaging

The STEM Images were taken for the nanocontainers produced by the BSA-Pectin conjugate having 2:1 m_{BSA}:m_{Pectin} weight ratio both using surfactant and without using surfactant. In addition to these, the nanocontainers produced by the BSA-Pectin conjugate 2:1 m_{BSA}:m_{Pectin} weight ratio with surfactant was syringe filtered to purify the sample and also the image of the filtered sample was taken. As shown in the Figure 4.5 the nanocontainers produced with surfactant having the size range from 160 nm to 350 nm. The Figure 4.7 shows the syringe filtered form of the same sample with 130 nm and 300 nm size range. These results show that the syringe filtration process is effective to eliminate the nanocontainers having higher size. On the other hand, Figure 4.6 shows the nanocontainers produced without using surfactant having a size range between 140 nm and 380 nm. The results with these size ranges can be acceptable because of there were high PDI value in the DLS measurement results of these samples. When the size range of the sample increases, the PDI value also increases. The results also show that the surfactant usage decrease the size of the produced nanocontainers. For these reasons, all these results are consistent with both the theoretical expectations and experimental results. The produced hollow nanocontainers show spherical shape contrary to expected ring like a shape. This can be originated from the difference in the electron scattering and transmission behavior of the used materials.

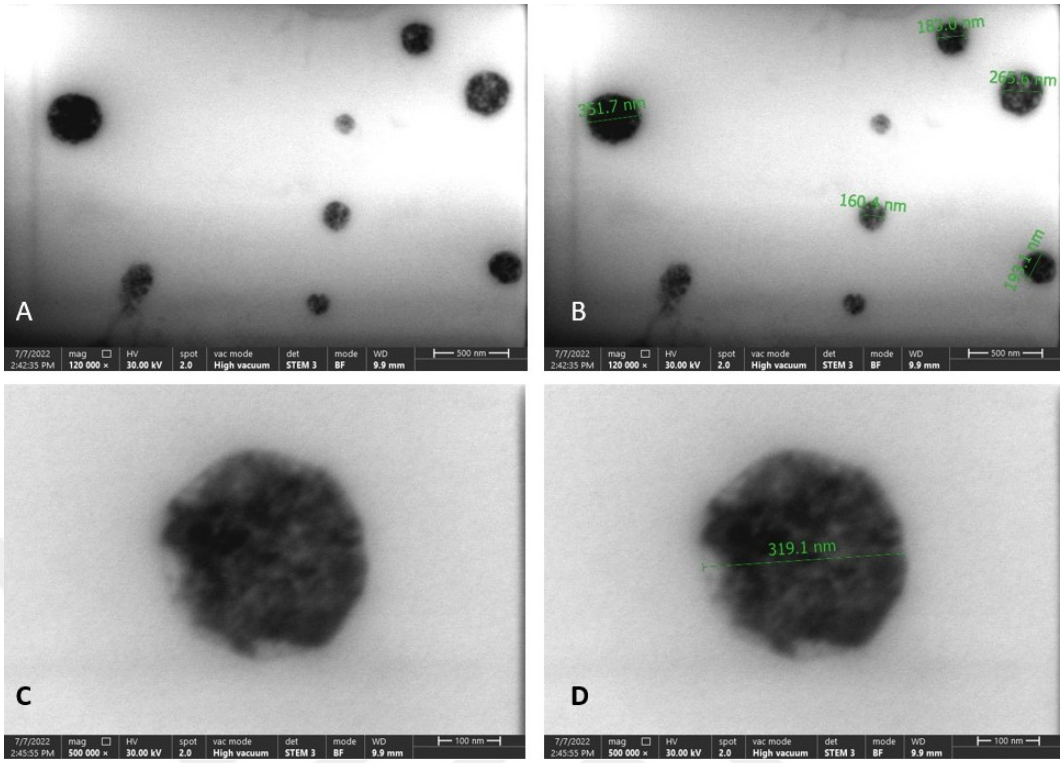

Figure 4.5 STEM Images of the nanocontainers produced with BSA-Pectin conjugate having 2:1 m_{BSA}:m_{Pectin} weight ratio prepared with pH adjustment by using surfactant A) Scale; 500 nm B) Scale; 500 nm size measurements C) Scale; 100 nm D) Scale; 100 nm size measurement.

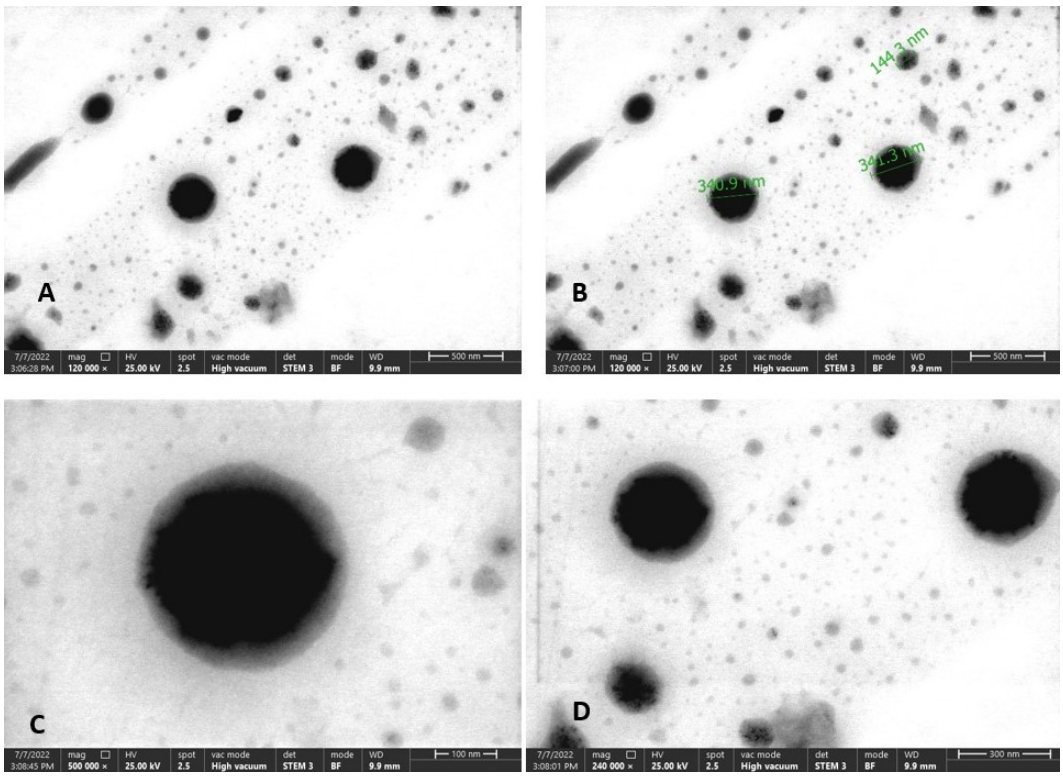

Figure 4.6 STEM Images of the nanocontainers produced with BSA-Pectin conjugate, having 2:1 m_{BSA}:m_{Pectin} weight ratio prepared with pH adjustment without using surfactant. A) Scale; 500 nm B) Scale; 500 nm size measurements C) Scale; 100 nm D) Scale; 300 nm.

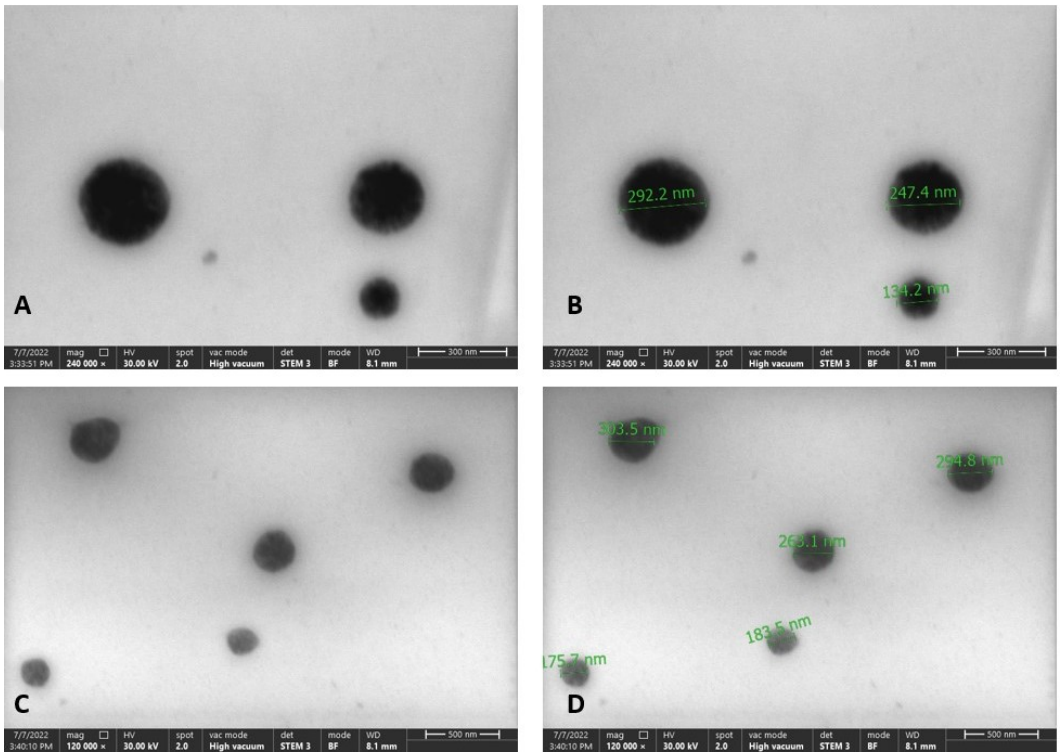

Figure 4.7 STEM Images of the syringe filtered nanocontainers produced with BSA-Pectin conjugate having 2:1 m_{BSA}:m_{Pectin} weight ratio prepared with pH adjustment by using surfactant. A) Scale; 300 nm B) The same scale with size measurements C) Scale; 500 nm D) Scale; 500 nm size measurements.

5. CONCLUSIONS AND OUTLOOK

5.1 Conclusions

Polymeric nanocontainers consist of both a core including some drugs, proteins and polymeric shell covering the core. The nanocontainers have an important role in the controlled drug delivery systems. Thanks to the shell of the nanocontainers, the living environment is protected from the harmful effects of the drugs and other cargo molecules placed into the core. Therefore, nanocontainers are used to treat diseases whose traditional treatment methods contain many side effects. Additionally, the membrane of the nanocontainers makes them more durable in the extreme conditions in terms of pH, heat or enzymatic activity. There are various types of polymeric materials that can be used to produce polymeric nanocontainers. Moreover, combinations of different polymers are suitable for the production of the polymeric nanocontainers. The main goal of this study was producing totally biocompatible, biodegradable, durable, hollow nanocontainers that consist of polymeric shell and lipid core. For these reasons, initially conjugates combined from the Bovine Serum Albumin and Pectin were produced by using Maillard reaction. The produced conjugates were characterized by using protein assay, SDS-PAGE and FT-IR methods. Secondly, the nanocontainers were produced with oil-in-water miniemulsion system. The nanocontainers were characterized by using Dynamic Light Scattering, Zeta Potential measurements and STEM imaging. The results of these studies were given below in order.

1. According to the results of the protein assay studies, there was a consistence between the expected and calculated protein amounts of the conjugates, and the most efficient one was the conjugate having 2:1 BSA-Pectin weight ratio.

2. The protein assay results showed that increase in the pH value of the conjugate preparation mixture does not negatively affect the used protein.

3. SDS-PAGE results proved that the conjugation was occurred in each BSA-Pectin

weight ratio.

4. FT-IR results confirmed the complexation of the BSA and Pectin. Furthermore, the additional peak around the secondary amide region showed that increasing in the pH of the conjugate production mixture improves the quality of the conjugation.

5. The DLS measurements revealed that the surfactant usage strongly effective to decrease the size of the produced nanocontainers.

6. The same measurements showed that increasing the BSA ratio in the conjugate directly decreases the size of the produced nanocontainers in case of surfactant free synthesis. The reason behind this was that the amphiphilic feature of the BSA.

7. The DLS measurements showed that the nanocontainers prepared with the conjugate having 2:1 BSA-Pectin weight ratio by using surfactant have smaller size and acceptable size distribution.

8. The nanocontainers produced with the conjugate having 2:1 BSA-Pectin weight ratio was selected for the further studies by considering the results of both the conjugate characterization studies and the DLS measurements.

9. The DLS measurements also unveiled that the nanocontainers prepared with the conjugates produced by increasing the pH (pH 8.3) have smaller sizes. This also means that increasing the pH of the conjugate preparation mixture improves the quality of the Maillard reaction, so the conjugates serve better emulsifier feature.

10. The DLS measurements of the nanocontainers prepared with higher conjugate concentration indicated that increasing the concentration does not linearly decrease the size and size distributions of the nanocontainers.

11. The other DLS measurements performed on the nanocontainers processed with centrifugation showed that the process does not effective to decrease size and size distribution of the nanocontainers.

12. The DLS measurements made on the syringe filtered nanocontainers revealed that syringe filtration is the best purification method to decrease size and size distribution of the nanocontainers.

13. STEM images supported the DLS measurement results in terms of nanocontainers size and size distribution.

5.2 Outlook

In the future, it is possible to conduct additional researches on the nanocontainers produced in this thesis study. The best storage condition of them can be investigated by making comparison between the solid and liquid form of the produced nanocontainers. The produced nanocontainers consists of both polymeric shell made up from the BSA-Pectin conjugates and oily core has a potential for the drug delivery studies in the future. Their drug loading, release profile can be investigated within these studies. In addition to these, cellular toxicity studies can be conducted by using the BSA-Pectin based nanocontainers. Moreover, additional advanced characterization microscopy techniques such as Cryogenic Transmission Electron Microscopy can be conducted for studying core/shell structure of the nanocontainers in a more detailed way in future studies.

REFERENCES

1. Zielinska A., Carreiró F. and Oliveira A.M., "Polymeric Nanoparticles: Production, Characterization, Toxicology and Ecotoxicology", *Molecules*, Vol. 3731, 6 2020.

2. Vert, M., Doi, Y. and Hellwich, K.H, "Terminology for biorelated polymers and applications (IUPAC Recommendations 2012)", *Pure Appl. Chem*, Vol. 84, jul-Sep. 2012.

3. Kluver, W., "Polymeric nanocapsules: An emerging drug delivery system", *J Adv Pharm Technol Res*, Vol. 3, jul-Sep. 2018.

4. İyisan B. and Landfester K., "Modular Approach for the Design of Smart Polymeric Nanocapsules", *Macromol. Rapid Commun.*, Vol. 40, jul-Sep. 2019.

5. Deng S., Gigliobianco R. and Censi R. , "Polymeric Nanocapsules as Nanotechnological Alternative for Drug Delivery System: Current Status, Challenges and Opportunities", *Nanomaterials*, Vol. 10, p. 847, 2020.

6. Torchilin, V., *Handbook of nanobiomedical research : fundamentals, applications, and recent developments*, World Scientific Publishing Co., 2014.

7. Thassu D., Deleers M. and Pathak Y., *Nanoparticulate Drug Delivery Systems*, Informa Healthcare, 2007.

8. Quiñones J.P., Peniche H. and Penich C., "Chitosan Based Self-Assembled Nanoparticles in Drug Delivery", *Polymers*, Vol. 10, p. 235, 2018.

9. Wasiak I., Kulikowska A. and Janczewska M., "Dextran Nanoparticle Synthesis and Properties", *PLoS One.*, Vol. 11, p. 235, 2016.

10. DeFrates K., Markiewicz T. and Gallo P., "Protein Polymer-Based Nanoparticles: Fabricationand Medical Applications", *Int. J. Mol. Sci.*, Vol. 19, p. 235, 2018.

11. Zhao Z., Li Y. and Xie M.B., "Silk Fibroin-Based Nanoparticles for Drug Delivery", *Int. J. Mol. Sci.*, Vol. 16, p. 235, 2015.

12. Deepmala KM., Singh VK., Chauhan S. and Jain N., "Soy Protein Based Green Composite: A Review", *Research Reviews: Journal of Material Sciences*, Vol. 16, p. 235, 2015.

13. Machado R., Bessa P.C. and Reis L.R, "Elastin-Based Nanoparticles for Delivery of Bone Morphogenetic Proteins", *Nanoparticles in Biology and Medicine: Methods and Protocols, Methods in Molecular Biology*, Vol. 906, 2012.

14. Rajangam T. and Soo S.S, "Fibrinogen and fibrin based micro and nano scaffolds incorporated with drugs, proteins, cells and genes for therapeutic biomedical applications", *Int J Nanomedicine*, Vol. 8, p. 3641–3662, 2013.

15. Malekhosseini P., Alami M. and Khomeiri M., "Development of casein-based nanoencapsulation systems for delivery of epigallocatechin gallate and folic acid", *Food Sci Nutr.*, Vol. 7, p. 519–527, 2019.

16. Cardoso V.S., Quelemes P.V and Amorin A., "Collagen-based silver nanoparticles for biological applications: synthesis and characterization", *Journal of Nanobiotechnology*, Vol. 12, p. 36, 2014.

17. Kumari A., Yadav S.K. and Yadav S.C., "Biodegradable polymeric nanoparticles based drug delivery systems", *Colloids and Surfaces B: Biointerfaces*, Vol. 75, pp. 1–18, 2010.

18. Stecanella L.A., Taveira S.F. and Marreto R.N., "Development and characterization of PLGA nanocapsules of grandisin isolated from Virola surinamensis: in vitro release and cytotoxicity studies", *Applications of Polymeric Nanocapsules, Current Drug Discovery Technologies*, Vol. 8, 2011.

19. Diyanat M., Saeidian H., Baziar S. and Mirjafary Z., "Development and characterization of PLGA nanocapsules of grandisin isolated from Virola surinamensis: in vitro release and cytotoxicity studies", *Environmental Science and Pollution Research*, Vol. 26, p. 21579–21588, 2019.

20. Milovanovic S., Djuris J., Dapčević A. and Zizovic S.I., "Soluplus®, Eudragit®, HPMC-AS foams and solid dispersions for enhancement of Carvedilol dissolution

rate prepared by a supercritical CO2 process", *Polymer Testing*, Vol. 76, pp. 54–64, july 2019.

21. Zarrintaj P., Saeb M.R., Jafari S.H. and Mozafari M., *Compatibilization of Polymer Blends, Application of compatibilized polymer blends in biomedical fields*, Elsevier, 2020.

22. Tamanna N. and Mahmood N, "Food Processing and Maillard Reaction Products: Effect on Human Health and Nutrition", *Int J Food Sci.*, Vol. 526762, 2015.

23. Feiner, G., *Salami, Practical Science and Processing Technology*, Academic Press, 2016.

24. Lund M.N. and Ray C.R., "Control of Maillard Reactions in Foods: Strategies and Chemical Mechanisms", *J. Agric. Food Chem*, Vol. 65, p. 4537−4552, 2017.

25. Zhang Q., Ames M.J. and Smith R.D., "A Perspective on the Maillard Reaction and the Analysis of Protein Glycation by Mass Spectrometry: Probing the Pathogenesis of Chronic Disease", *Journal of Proteome Research*, Vol. 8, p. 754–769, 2009.

26. Oliveira F.C., Coimbra J.S. and Oliveira E.B., "Food Protein-polysaccharide Conjugates Obtained via the Maillard Reaction: A Review", *Crit Rev Food Sci Nutr*, Vol. 56(7), pp. 1108–25, 2016.

27. Koubaaa M. and Roohinejadb S., *Effect of Emerging Processing Technologies on Maillard Reactions*, Elsevier, 2018.

28. Ames, J., "Applications of the Maillard reaction in the food industry", *Food Chemistry*, Vol. 62, pp. 431–439, 1998.

29. Nursten H., *The Maillard Reaction Chemistry, Biochemistry and Implications*, he Royal Society of Chemistry, 2005.

30. Lee Y.Y., Tang T.K. and Phuah T.E. , "New functionalities of Maillard reaction products as emulsifiers and encapsulating agents, and the processing parameters: a brief review", *Journal of the Science of Food and Agriculture*, Vol. 97, 2017.

31. Rong X., Xie Y. and Hao X., "Applications of Polymeric Nanocapsules in Field of Drug Delivery Systems", *Current Drug Discovery Technologies*, Vol. 8, pp. 173–187, 2011.

32. Hickey R.J., Haynes A.S. and Kikkawa J.M., "Controlling the Self-Assembly Structure of Magnetic Nanoparticles and Amphiphilic Block-Copolymers: From Micelles to Vesicles", *J. Am. Chem. Soc.*, Vol. 133, p. 1517–1525, 2011.

33. Kamps A.C., Gaytan B.L. and Hickey R.J., "Nanoparticle-Directed Self-Assembly of Amphiphilic Block Copolymers", *Langmuir*, Vol. 26(17), p. 14345–14350, 2010.

34. J.Asua, "Miniemulsion polymerization", *Progress In Polymer Science*, Vol. 27-7, pp. 1283–1346, September 2002.

35. Kammari N., Das H.G. and Das S.K., *Emerging Nanotechnologies for Diagnostics, Drug Delivery, and Medical Devices*, Elsevier, 2017.

36. T.Peters, *All about Albumin: Biochemistry, Genetics, and Medical Applications*, Elsevier, 1995.

37. Moman R.N., Gupta N. and Varacallo M., *Physiology, Albumin*, StatPearls Publishing, 2022.

38. Topala T. and Bodokl A., "Bovine Serum Albumin Interactions with Metal Complexes", *Clujul Med.*, Vol. 87, p. 215–219, 2014.

39. Wang J. and Zhang B., "Bovine Serum Albumin as a Versatile Platform for Cancer Imaging and Therapy", *Current Medicinal Chemistry,*, Vol. 25, pp. 2938–2953, 2018.

40. Wang X., Zhang G. and Yu D., "The interaction of folate modified Bletilla striata polysaccharide based micelle with bovine serum albumin", *Glycoconjugate Journal*, Vol. 38, p. 585–597, 2021.

41. Bal W., Christodoulou J., Sadler P.J. and Tucker A., "Multi-metal binding site of serum albumin", *J. Inorg. Biochem.*, Vol. 70, pp. 33–39, 1998.

42. Flutto L., *PECTIN | Properties and Determination", Encyclopedia of Food Sciences and Nutrition*, Academic Press, 2003.

43. Smith D., *JAMS AND PRESERVES | Methods of Manufacture", Encyclopedia of Food Sciences and Nutrition*, Academic Press, 2003.

44. Zdunek A., Piotr M. and Cybulska J., "The primary, secondary, and structures of higher levels of pectin polysaccharides", *Compr Rev Food Sci Food Saf*, Vol. 20, p. 1101–1117, 2021.

45. Lipnizki F., "Basic Aspects and Applications of Membrane Processes in Agro-Food and Bulk Biotech Industries", *Comprehensive Membrane Science and Engineering*, Vol. 4, pp. 165–194, 2010.

46. Sticklen M., "Plant genetic engineering for biofuel production: towards affordable cellulosic ethanol", *Nature Reviews Genetics*, Vol. 4, pp. 433–443, 2008.

47. Mudgil, D., *Dietary Fiber for the Prevention of Cardiovascular Disease Fiber's Interaction Between Gut Micoflora, Sugar Metabolism, Weight Control and Cardiovascular Health*, Academic Press, 2017.

48. Vincken P., Borkhardt B. and Bush M., "Remodelling Pectin Structure In Potato", *Developments in Plant Genetics and Breeding*, Vol. 6, pp. 245–256, 2000.

49. Naqash F., Sajad F.A., Gani W.A. and Rather A., "Emerging concepts in the nutraceutical and functional properties of pectin—A Review", *Carbohydrate Polymers Volume*, Vol. 168, pp. 227–239, July 2017.

50. Khoder M., Gbormoi H.K. and Ryan A., "Potential Use of the Maillard Reaction for Pharmaceutical Applications: Gastric and Intestinal Controlled Release Alginate-Albumin Beads", *Pharmaceutics.*, Vol. 11(2):83, Feb 2019.

51. Rohiwal S.S., Ellederova Z. and Tiwari A.P., "Self-assembly of bovine serum albumin (BSA)– dextran bio-nanoconjugate: structural, antioxidant and in vitro wound healing studies", *RSC Adv.*, Vol. 11, p. 4308–4317, 2021.

52. Karseno E., Yanto T. and Setyowati R., "Effect of pH and temperature on browning intensity of coconut sugar and its antioxidant activity", *Food Research*, Vol. 2(1), pp. 32–38, Feb. 2018.

53. Chen H., Ji A and Qiu S., "Covalent conjugation of bovine serum album and sugar beet pectin through Maillard reaction/laccase catalysis to improve the emulsifying properties", *Food Hydrocolloids*, Vol. 76, 2018.

54. BeckerGuy J.M. and Zachgo A., *Biotechnology, A Laboratory Course*, Academic Press, 1996.

55. ThermoFisher Scientific, *Overview of Protein Assays Methods*, Jun. 2017.

56. Thermo Scientific, *Pierce 660nm Protein Assay*, 2018, rev. A.0 22660 22662.

57. Brunell J.L and Green R., "One-dimensional SDS-Polyacrylamide Gel Electrophoresis (1D SDS-PAGE)", *Methods in Enzymology*, Vol. 541, p. Elsevier, 2014.

58. Blancher C. and Jones A., "SDS-PAGE and Western Blotting Techniques", *Metastasis Research Protocols*, Vol. 1, 2001.

59. Intvitrogen, *Bolt™ Bis-Tris Plus Mini Gels*, Oct. 2018, rev. B.0 MAN0007902.

60. Intvitrogen, *4X Bolt™ LDS Sample Buffer*, May 2022, rev. A.0 B0007.

61. Intvitrogen, *10X Bolt™ Sample Reducing Agent*, May 2022, rev. A.0 B0004.

62. Intvitrogen, *20X Bolt™ MES SDS Running Buffer*, May 2022, rev. A.0 B0002.

63. Intvitrogen, *Mini Gel Tank User Guide*, 2018, rev. C.0 MAN0010862.

64. Intvitrogen, *SimplyBlue™ SafeStain*, Feb. 2012, rev. C.0 LC6060.

65. Mohamed M.A., Jaafar J. and Ismail A.F., "Fourier TransformInfrared (FTIR) Spectroscopy", *Membrane Characterization*, pp. 3–29, 2017.

66. Kowalczuk D. and Pitucha M., "Application of FTIR Method for the Assessment of Immobilization of Active Substances in the Matrix of Biomedical Materials", *Materials (Basel)*, Vol. 12(18): 2972, Sep. 2019.

67. Nakama Y., "Characteristics and Classification of Surfactants", *Cosmetic Science and Technology*, 2017.

68. Jiang B., Hu L., Gao C. and Shen J., "Crosslinked polysaccharide nanocapsules: Preparation and drug release properties", *Acta Biomaterialia*, Vol. 4(1), pp. 9–18, 2006.

69. Rollett A., Reiter T. and Nogueira P., "Folic acid-functionalized human serum albumin nanocapsules for targeted drug delivery to chronically activated macrophages", *International Journal of Pharmaceutics*, Vol. 427, pp. 460–466, May. 2012.

70. Pereira A.S., Tavares P. and Vieira P.L, "Dynamic Light Scattering (DLS)", *Radiation in Bioanalysis*, Vol. 8, pp. 173–193, 2019.

71. Stetefeld J., McKenna S.A. and Trushar R., "Dynamic light scattering: a practical guide and applications in biomedical sciences", *Biophys Rev.*, Vol. 8(4), p. 409–427, Dec. 2016.

72. WeiLu G. and Gao P., *Handbook of Non-Invasive Drug Delivery Systems Non-Invasive and Minimally-Invasive Drug Delivery Systems for Pharmaceutical and Personal Care Products Personal Care Cosmetic Technology*, Elsevier, 2010.

73. Selvamani V., *Characterization and Biology of Nanomaterials for Drug Delivery Nanoscience and Nanotechnology in Drug Delivery Micro and Nano Technologies*, Elsevier, 2019.

74. Shibata N., Kohno Y. and Findlay S.D., "New area detector for atomic-resolution scanning transmission electron microscopy", *Journal of Electron Microscopy*, Vol. 59(6), p. 473–479, Dec. 2010.

75. Albert V., "Special Invited Review Scanning transmission electron microscopy", *Journal of Electron Microscopy*, Vol. 100, pp. 247–259, Apr. 1974.

76. ThermoFisher Scientific, *Electron microscopes: https://www.thermofisher.com/tr/en/home/electron-microscopy/products.html*.

77. Varela M., Lupini A.R. and Benthem K., "Materials Characterization In The Aberration-Corrected Scanning Transmission Electron Microscope", *Annu. Rev. Mater.*, Vol. 35, pp. 539–569, 2005.

78. Candraningrum R., Setiowati A. and Hidayat C., "Electrostatic-Maillard formation of coconut protein Concentrate-Pectin conjugate for Oil-in-Water Emulsion: Effects of Ratio, Temperature, and pH", *Journal of the Saudi Society of Agricultural Sciences*, 2022.

79. Baler K., Martin O.A. and Carignano M.A, "Electrostatic Unfolding and Interactions of Albumin Driven by pH Changes: A Molecular Dynamics Study", *J Phys Chem B*, Vol. 118(4), p. 921–930, Jan. 2014.

80. Estey T., Kang J., Schwendeman S.P. and Carpenter J.F., "BSA degradation under acidic conditions: a model for protein instability during release from PLGA delivery systems", *J Pharm Sci.*, Vol. 95(7), pp. 1626–1639, Jul. 2006.

81. Raghuwanshi V.S., Yu B., Browne C. and Garnier G., "Reversible pH Responsive Bovine Serum Albumin Hydrogel Sponge Nanolayer", *Front. Bioeng. Biotechnol.*, Jun. 2020.

82. Pavia D.L., Lampman G.M., Kriz G.S. and Vyvyan J.A., "Introduction to spectroscopy a guide for students of organic chemistry", *CenGaGe Learning*, 2015.

83. Nandiyanto D., Oktiani R. and Ragadhita R., "How to Read and Interpret FTIR Spectroscope of Organic Material", *Indonesian Journal of Science Technology*, Vol. 4(1), pp. 97–118, 2019.

84. Burova T., Grinberg V., Valerij Y., Tolstoguzov B. and Kruif G., "Conformational Changes in - and K-Carrageenans Induced by Complex Formation with Bovine â-Casein", *Biomacromolecules*, Vol. 8, pp. 368–375, 2007.

85. Gawkowska D., Cybulska J. and Zdunek A., "Structure-Related Gelling of Pectins and Linking with Other Natural Compounds: A Review", *Polymers (Basel)*, Vol. 10(7), p. 762, july 2018.

86. Esmaeili A., Rahnamoun S. and Sharifnia F., "Effect of O/W process parameters on Crataegus azarolus L nanocapsule properties", *Journal of Nanobiotechnology*, Vol. 11, pp. 460–466, May. 2013.

APPENDIX A. CALIBRATION CURVE FOR PROTEIN ASSAY

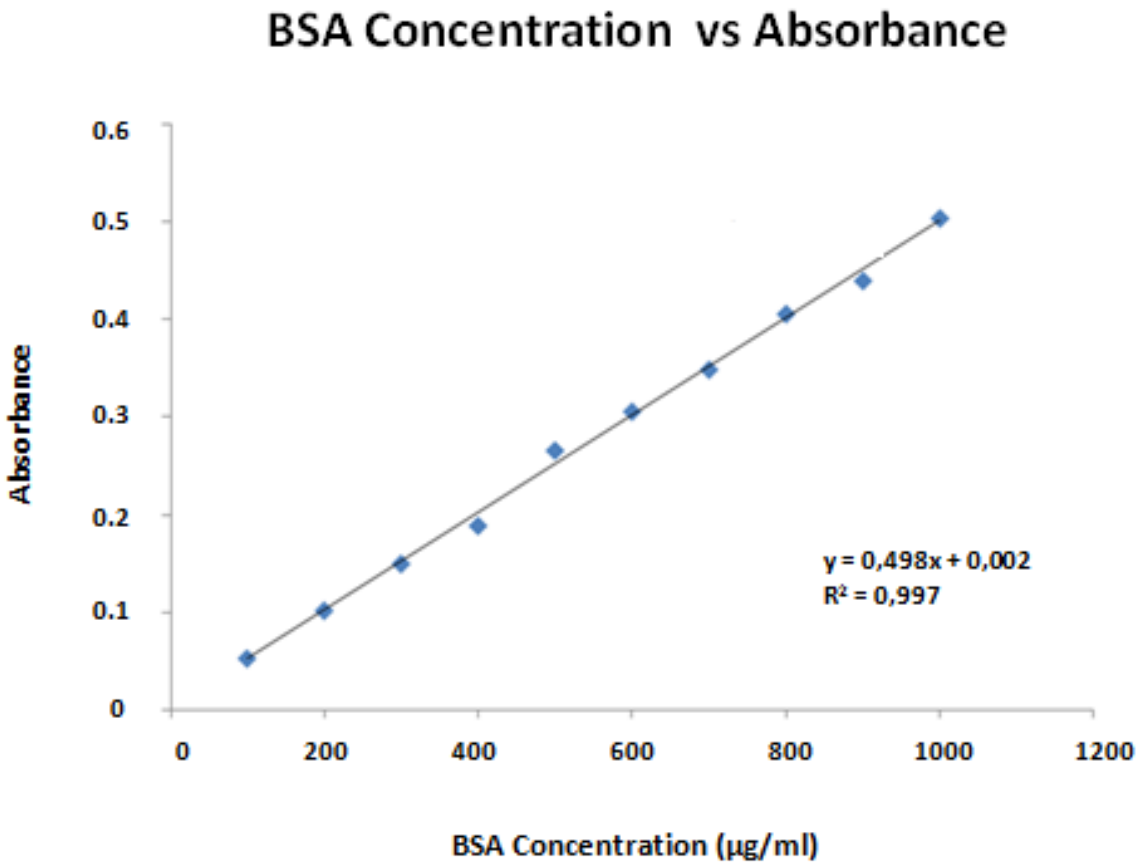

Figure A.1 Generated Calibration Curve at $\lambda = 655$ nm by using solutions having different BSA concentration to determine the BSA contration in the produced BSA-Pectin conjugates.